MODELING, SIMULATION & CONTROL OF DIRECTIONAL STEERING SYSTEM

BY

MOHAMMAD TALIB

A Thesis Presented to the

DEANSHIP OF GRADUATE STUDIES

KING FAHD UNIVERSITY OF PETROLEUM & MINERALS

DHAHRAN, SAUDI ARABIA

In Partial Fulfillment of the
Requirements for the Degree of

MASTER OF SCIENCE

In

SYSTEMS ENGINEERING

NOVEMBER 2013

KING FAHD UNIVERSITY OF PETROLEUM & MINERALS

DHAHRAN- 31261, SAUDI ARABIA

DEANSHIP OF GRADUATE STUDIES

This thesis, written by **MOHAMMAD TALIB** under the direction of his thesis advisor and approved by his thesis committee, has been presented to and accepted by the Dean of Graduate Studies, in partial fulfillment of the requirements for the degree of **MASTER OF SCIENCE IN SYSTEMS ENGINEERING.**

Dr. Moustafa El Shafei
(Advisor)

Dr. Abdul-Wahid A. Saif
(Member)

Dr. Samir Al-Amer
(Member)

Dr. Fouad M Al Sunni
Department Chairman

Dr. Salam A. Zummo
Dean of Graduate Studies

13/2/14
Date

Dedicated to my beloved parents and brothers

ACKNOWLEDGMENTS

All praise to Almighty Allah and his beloved messenger Muhammad (SAWS). My thanks to King Fahd University of Petroleum and Minerals for providing a great environment for education and research. I would also like to thank the King Abdulaziz City for Science and Technology (KACST) for financial support through research project KACST AR30-258 2012-14.

I extend my heartfelt gratitude to my thesis advisor Dr. Moustafa El Shafei for his continuous support, patience and encouragement. He stood by me in all times and was the greatest support I had during my tenure in the university and most importantly during my thesis. I would also like to thank my thesis committee Dr. Abdul-Wahid A. Saif and Dr. Samir Al-Amer for their time and valuable comments. I also extend my gratitude to Dr. Fouad Al Sunni, the chairman of Systems Engineering Department for his support throughout my tenure at KFUPM.

I would like to acknowledge my parents for their everlasting love, trust and faith in me and providing me the finest things I ever needed. I could never have pursued my higher education without their encouragement and support. My brothers who have always loved and supported me in all forms of life, their love gives me immense strength to keep moving ahead in all forms of life.

Lastly I would like to thank all my friends and colleagues back at home and at KFUPM whose presence and discussions were biggest support during the times of loneliness and despair.

TABLE OF CONTENTS

LIST OF TABLES

LIST OF FIGURES

LIST OF ABBREVIATIONS

BHA	:	Bore Hole Assembly
DSS	:	Directional Steering System
FoB	:	Force on Bit
FLC	:	Feedback Linearization Controller
LQR	:	Linear Quadratic regulator
MWD	:	Measurement While Drilling
MPD	:	Managed Pressure Drilling
PDM	:	Positive Displacement Motor
RSS	:	Rotary Steerable Systems
RoP	:	Rate of Penetration
RPM	:	Revolution per Minute
RCD	:	Rotating Control Device
WoB	:	Weight on Bit

NOMENCLATURE

RoP = Rate of Penetration, ft/hr

D_S = Block Position, ft

Time = Time, hr

WoB = Weight on Bit, lbs

Torque = Torque, $ft - lbs$

Bit Diameter = Bit Diameter, ft

K = Elasticity Coefficient of Drill-String, ft/lbs

L = Length of Drill-String, ft

E = Modulus of Elasticity, psi

RPM = Rotary Speed, rev/min

α_k = King's Parameters, ft/hr

β_1, β_2 = King's Parameters, dimensionless

β_3 = King's Parameters, $ft/hr/lbs$

T_{Dim} = Dimensionless Torque

$FORS$ = Apparent Formation Strenght, psi

R_D = Dimensionless RoP

σ = Compressive Strength, psi

$EFFM$ = Energy Efficiency of Drilling, psi

$EFFS_{Mmin}$ = Minimum Energy Efficiency of Drilling, psi

μ = Bit-Specific Coefficient of Sliding Friction, dimensionless

Axial Force = Axial Force, lbs

Depth of Cut = Depth of Cut, in/rev

R_f = Force Ratio, dimensionless

ABSTRACT

Name : Mohammad Talib

Thesis Title : Modeling, Simulation and Control of Directional Steering System

Major Field : Systems Engineering

Date of Degree : November 2013

Directional Steering Systems (DSS) have been developed in the oil and gas industry to achieve high well production when compared to conventional drilling systems. In this thesis a dynamic modeling of a DSS using four motors was developed. A controller was designed using Feedback Linearization technique for the cancellation of non-linear dynamics and LQR for the optimal linear control. Simulation of the proposed 4-motors DSS is provided, and the performance of the Feedback Linearization Controller (FLC) – Linear Quadratic Regulator (LQR) based command and control in executing steering tasks is demonstrated.

ملخص الرسالة

الاسم الكامل: محمد طالب

عنوان الرسالة: نمذجة ومحاكاة وتحكم في نظام توجيه إتجاهي

التخصص: هندسة النظم

تاريخ الدرجة العلمية: محرم 1435

تم تطوير أنظمة التوجيه الاتجاهية (DSS) في صناعة النفط والغازللحصول على آبار ذات إنتاج عالي بالمقارنة مع أنظمة الحفر التقليدية. في هذه الأطروحة تم تطوير نماذج ديناميكية لنظم توجيه اتجاهية باستخدام أربعة محركات. تم تصميم متحكم باستخدام طرق التحويل الى نظام خطي باستخدام التغذية الخلفية (FLC) و ذلك لالغاء الديناميكية غير الخطية و تم استخدام التحكم الخطي الأمثل (LQR) لتصميم نظام تحكم خطي. تمت محاكات نظام التوجيه الاتجاهي المقترح كما تم دراسة اداء التحويل الى نظام خطي باستخدام التغذية الخلفية (FLC)ونظام التحكم المعتمد على التحكم الخطي الأمثل (LQR) للقيام بمهمات التحكم في الاتجاه .

CHAPTER 1

INTRODUCTION

1.1 General Description

Directional Drilling is the process of directing the wellbore along some trajectory to a predetermined target [1]. Directional Steering System (DSS) has a significant importance in the oil and gas industry because it achieves high well productivity. DSS facilitates the accessibility of the oil reservoir in complex locations, and enables if the reservoir is having large surface area and distributed over thin horizontal layer. Horizontal drilling yields higher productivity when compared to conventional vertical drilling because horizontal wells have larger contact area with oil and gas reservoir's [2]. Wells are also drilled directionally for several purposes like allowing more well heads to be grouped together on one surface location, drilling along the underside of a reservoir-constraining fault, and allows production from multiple layers.

DSS has substantially reduces the cost of the drilling operations and the total amount of cost [3]. Thus, the development of the Directional Steering mechanisms for drilling operations have gained more attention and become one of the major area of research in Oil and Gas Industry.

In 1930's the first controlled directional well was drilled at Huntington Beach, California. Till 1950's whipstock's and bit jetting techniques were employed for drilling directional wells. In 1960's the first commercial Positive Displacement Motor (PDM) was used for directional drilling. The PDM is constructed with a bent housing to provide a side force to the bit and to deflect the hole trajectory. The major advance was in 1970's when down-hole drilling motors were become common. In 1980's witnessed the first use of Measurement While Drilling (MWD) tool to provide continuously updated measurements. In 1999 a Rotary Steerable System (RSS) introduced to directional drilling markets. RSS was one of the advance method in directional drilling which allow three dimensional control of a bit without stopping the drill string rotation, increased the efficiency of directional drilling operations by reducing drilling time. It also provides better borehole cleaning with fewer wiper trips, optimizes drilling parameters, and provides a higher rate of penetration while drilling [4].

To ensure proper directional drilling, the driller must have complete knowledge of the drill bit direction and orientation of drilling process. Directional drillers are given preplanned well path to follow that is determined by engineers and geologists before the drilling commences. Unlike conventional drilling systems, the directional drilling require position sensors to provide survey data of the well bore. It provides estimations of the azimuth ψ (deviation from the north direction in the horizontal plane), the inclination θ (deviation from the vertical direction, or pitch angle), and the tool face angle ϕ (roll angle) of the drill bit [3]**.**

The directional drilling system includes MWD tool, a steering system and a drilling assembly. The position sensors which take measurements at regular intervals between 30-500 feet , with 100 feet common during active changes of angle or direction is also a part of MWD. The drilling head assembly consists of a bit, a high-speed motor, nonmagnetic drill collars, and a drill pipe. The nonmagnetic drill collar holds the surveying equipment. After drilling a vertical hole to an appropriate depth then the directional steering procedure begins. The drill head assembly is then installed in the hole. The Bore Hole Assembly (BHA) is directed toward the desired offset angle (azimuth direction) using the adjustable housing in a PDM motor. The offset angle is usually 1.5 degrees, with a maximum of 3 degrees [5]. Three- axis magnetometers and three-axis accelerometers are used to determine the azimuth, the inclination and tool face angle. Corrections are regularly made by adjusting rotation speed or the Weight on Bit (WoB).

1.2 Problem Formulation

Drilling is very slow process with rates of penetration ranging from 0.1 to 500 m/hr. The curvature at which directional course changes can be imposed on the well-path made is also low, being much less than $15°$ for every 30 m drilled on average. Drilling does not necessarily follow the intended trajectory. Something happens downhole which makes the drill-string deviate from its course. For corrective runs it takes lot of non-productive time. The main challenge of directional driller is to set the specific tool face orientation accurately by experimenting the WoB and top drive quill position. The main task is to properly orientate the downhole tool to steer the well bore in a desired direction. In order to achieve this the driller has to work with throttles, clutches, brakes and a forward or

reverse control to orient the drill pipe to correct the position, which makes the drilling procedure very complicated, time consuming and expensive for monitoring and correcting the direction of the drilling head.

After performing a literature review it was found that there are open research areas in the directional steering of the drill head assembly and to design a controller for the directional steering technique.

1.3 Objectives

The aim of this thesis is to develop a model for the Directional Steering System consists of four motors driving four drilling bits in order to alleviate the complicated, time consuming and expensive procedure of directional drilling.

The use of four motors and four drill bits allow precise steering of the head by independently controlling the speed of each bit. Thus, the objectives of the thesis are:

1. To develop a dynamic model of drilling head assembly consists of four motors and
2. Development of a control method to precisely follow the desired trajectory.

1.4 Proposed Approach

The goal of the thesis is to develop the dynamic model of the DSS and control method to precisely follow the desired trajectory. The work involves:

- Studying the drilling process to better understand the objective and the importance of the various process variables.
- Studying the factors that effecting the drill bit performance.

- To identify the characteristics of rock-bit interaction and to propose equations required for the control of top drive power and torque of the motors.
- To develop steering mechanism for the four motor DSS.
- Identification of the appropriate control technique for the DSS model.
- Development of controller for the DSS.
- Simulation of results to check the performance of controller.

1.5 Thesis Organization

The thesis is organized as follows. Chapter 2 deals with the literature review. The modeling of DSS is covered in chapter 3. In Chapter 4, the control design is presented and the proposed controller is evaluated by tracking the desired trajectory, and Chapter 5 concludes the thesis work and presents a few future extensions.

CHAPTER 2

LITERATURE REVIEW

2.1 Factors effecting DSS Performance

Several factors such as rock characteristics, bottom-hole confining and wellbore pressure, bit design and condition, mud composition, hydraulics, and bit operating parameters that influence on the DSS performance.

2.1.1 Rock Characteristic's [1]

Rate of Penetration (RoP) was affected by the elastic limit and the formation strength of the rock. However, RoP can be changed by the mineral composition. For example, rocks containing gummy clay can cause the bit to ball up and abrasive minerals can cause rapid dulling of the bit teeth.

2.1.2 Bottom-Hole Confining and Wellbore Pressure [3]

The rocks strength is related to the effective confining stress on the rock. Furthermore, the difference between wellbore pressure and pore pressure is generally accepted as the effective confining stress. As confining stress increases, both the stress and strain to fail the rock increase. The increase in strain to failure increases the work required to fail the rock. Consequently, when the difference between the well-bore pressure and the pore pressure increases, RoP decreases.

2.1.3 Bit Design and Condition [4]

The bit type selected and the design characteristics of the bit have a significant influence on RoP and effectiveness for the specific rock. Tooth length; number of cutters; cutter exposure or blade standoff; size, shape, surface, and angle of the cutter; and nozzle and jet design are some of the many bit characteristics which affect RoP and bit performance. Bit condition, specifically the bit wear state, has influence on the effectiveness of drilling, and increased wear reduces RoP and bit performance.

2.1.4 Mud Composition [5]

The properties of the drilling fluid highly affect RoP. Density, rheological flow properties, filtration characteristics, solids content and size distribution, and chemical composition are some of the properties which have a high influence on bit performance.

2.1.5 Bit Operating Parameters [2-9]

Weight on bit (WoB): Weight on bit (WoB), is amount of the axial force applied to the bottom-hole formation to break the rock by the bit. It is calculated based on the difference between the measured weight of drill-string at the surface during off-bottom rotation and during the drilling operation. Typically, a plot of RoP vs. WoB, obtained experimentally with all other drilling variables held constant, will have the characteristic shape shown in Figure 2.1, no significant RoP is obtained until the threshold WoB is applied. Then, the penetration rate increases rapidly with increasing WoB for moderate values of WoB, and at higher values of WoB, only small improvements in RoP are observed. Finally, at extremely high values of WoB, RoP no longer increases. Despite of increasing WoB, this

behavior often is called bit floundering, and the point of maximum RoP is called flounder point. The poor response of RoP at high values of WoB is usually attributed to less efficient bottom-hole cleaning.

In shale, increasing WoB more than flounder point decreases RoP and "after flounder point, RoP is insensitive to WoB." As shown Figure 2.2, in the situation of balling after WoB past flounder point, the bit starts to ball up and become ineffective, so the previous RoP is not achievable anymore.

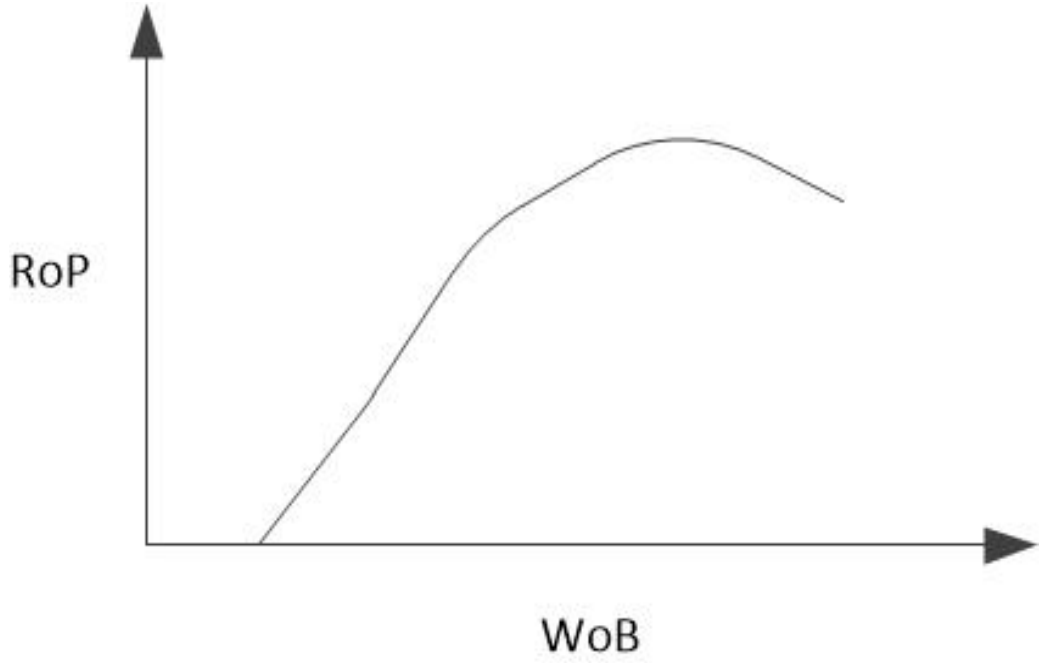

Figure 2.1: RoP vs. WoB (normal Condition)

Rotary Speed: When all other drilling variables are held constant, RoP usually increases with RPM at low values. At higher values of RPM, the response of RoP to increasing RPM diminishes. The poor response of RoP at high values of RPM usually is attributed to less efficient bottom-hole cleaning. In addition to previous information, choosing the appropriate WoB and RPM is highly influenced by types of rocks. For example, usually

weak rocks drill with low WoB and high RPM, and strong rocks drill best with high WoB and low RPM. Also, low RPM increases the chance of stick slip, so the moderate RPM is preferred.

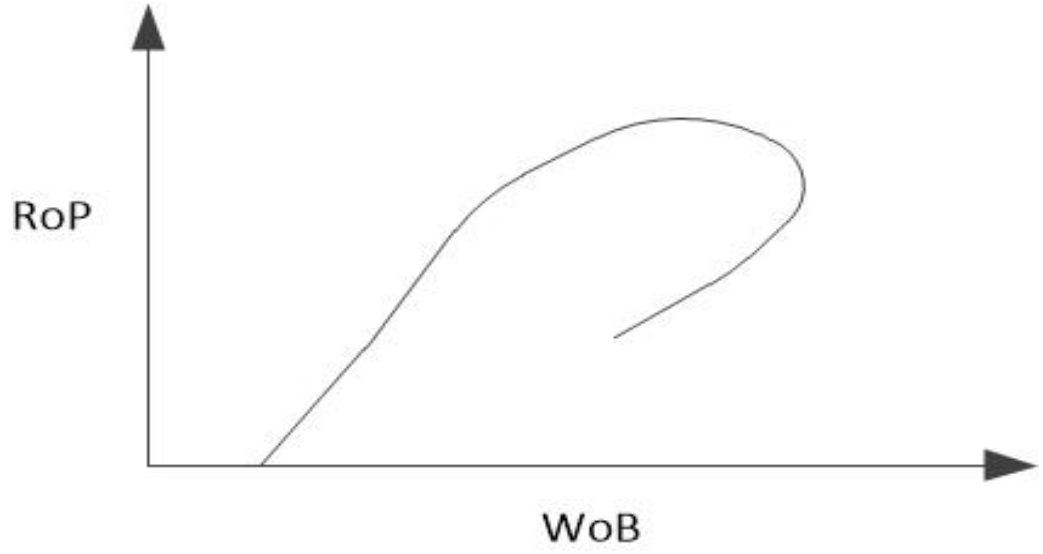

Figure 2.2: RoP vs. WoB (Balling)

Hydraulics: Increasing bit hydraulics and flow rate is widely considered to have a significant influence on RoP. The level of hydraulics achieved at the bit affects the flounder point of the bit. A flounder point is reached eventually when the cuttings are not removed as quickly as they are generated, so if the level of hydraulics is increased, a higher RoP will be achieved at the new bit flounder point.

2.2 Relationship between Surface Data and Bottom-Hole Data [1-4]

2.2.1 WoB, Torque, and RPM

WoB is calibrated during the connection time before start of drilling to zero and hook load at surface set as the origin, then during drilling, difference between actual hook load

and the original one defines the actual WoB. Torque is typically measured using the electric current delivered to the rotary table or the top drive. RPM is measured by a rotary table RPM sensor.

2.2.2 Rate of Penetration (RoP)

The conventional rate of penetration instrumentation does not provide a correct measurement indicating the progress of the bit. It measures merely the progress of the downward motion of the upper end of the drill string by measuring block or drill line travel.

However, the drill string is continuously subjected to variation of length due to elastic deformations and dynamics of the drill string, so the motion of the block is not the same as the motion of the bit. In order to eliminate the errors resulting from a lack of allowance made for the elastic variations in the length of the drill pipe, the rate of drilling penetration is usually determined by the average value of the drilling rate over an appreciable depth or time. Several approaches are proposed to calculate rate of penetration more accurately, and some of them will be introduced.

2.2.3 Arthur Lubinski, 1949 [14]

Because the length of the drill string is affected by the change in forces due to elastic deformations, this approach assumed that the change in the drill-string length is equal to a linear function of the change in force due to the change in weight on bit, assuming the drill string behaves as a perfect spring [11]. As

shown in Equations 2.1 and 2.2, the speed of drilling at the bit, RoP, is equal to the sum of the change in length of drill string, which is proportional to the change in WoB, the elasticity coefficient of the drill string, and block speed at surface. This method neglected the effects of the dynamics of the drill string and of friction between the hole and drill string.

$$RoP = \frac{dD_s}{dTime} + K\frac{dWoB}{dTime} \tag{2.1}$$

$$K = L/144EA \tag{2.2}$$

2.2.4 Yves Kerbart, 1989 [15,16]

Yves Kerbart's method creates an empirical basis for Lubinski's method [14]. It calculates the elasticity coefficient of the drill string by using a statistical model of previous drilling operation data based on assumptions that the lithology does not change and the rate of penetration remains constant. As shown in Equations 2.3 and 2.4, the elasticity coefficient (K) is calculated from a linear regression of change in WoB and the difference between block speed and long-term RoP. Then a corrected RoP was calculated by using the calculated K in Lubinski's equation.

$$\left[RoP_L - \frac{dD_S}{dTime}\right] = K_{kerbart}\frac{dWoB}{dTime} \tag{2.3}$$

$$RoP = \frac{dD_S}{dTime} + K_{kerbat}\frac{dWoB}{dTime} \tag{2.4}$$

2.3 Methods to Diagnose Performance Problems

2.3.1 I.G. Falconer et al., 1988 [17]

This research uses down-hole torque and WoB to calculate dimensionless torque as shown in Equation 2.5 and apparent formation strength (FORS), Equation 2.6 in a method to separate the bit effects from the lithology effects during drilling. "Dimensionless torque, T_{Dim}, is proportional to the bit efficiency and the ratio for the in-situ shear strength to the in-situ penetration strength. Apparent formation strength, FORS, is proportional to the in-situ penetration strength of the rock and inversely proportional to the bit efficiency.

$$T_{Dim} = \frac{Torque}{(WOB * Bit\ Diameter)} \tag{2.5}$$

$$FORS = \frac{(5 \times WOB * RPM)}{12 \times RPM * Bit\ Diameter} \tag{2.6}$$

if R_D, dimensionless RoP, is used:

$$R_D = \frac{ROP}{(60 * RPM * Bit\ Diameter)} \tag{2.7}$$

$$FORS = \frac{(WOB)}{144 * R_D * (Bit\ Diameter)^2} \tag{2.8}$$

As shown in Figure 2.3, the research separates different situations based on these two proposed diagnostic parameters. Many field case studies have been done to examine the

effects of lithology changes on the drilling response. They claim that the techniques can provide:

1. Rock strength and lithological correlation (classified into three categories: porous, argillaceous (shaly), and tight, corresponding to high, medium and low torque respectively),

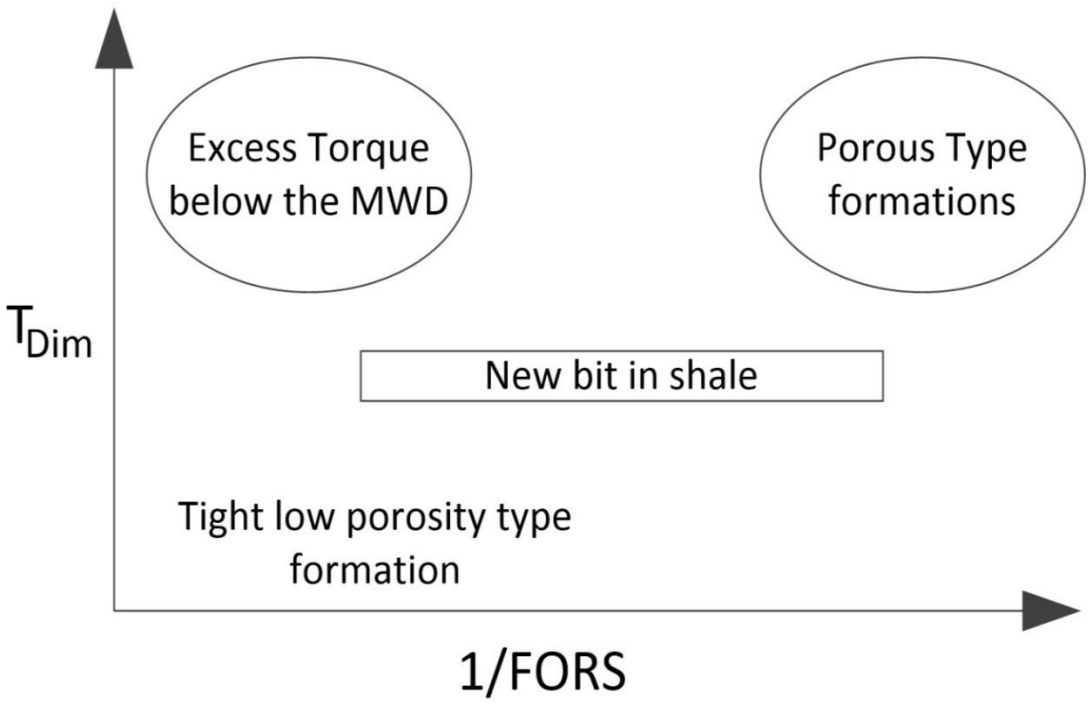

Figure 2.3: Falconer's Diagnosis

2. Wear state of the bit teeth in shales (using trends in bit torque and rate of penetration in shale type formations to separate the wear of milled tooth and PDC bits from changes in shale strength, and reaching the conclusion that it was not possible to interpret bit wear in non-shale type formations),
3. Excessive torque and cone locking, and

4. Insensitivity of surface drilling measurements to major formation changes (e.g. sand/shale boundaries), particularly in deviated wells.

2.3.2 R.C. Pessier et al., 1992 [19, 20]

This research study uses a comparison between full-scale simulator tests and field data to develop an energy-balanced model for drilling under hydrostatic pressure. Using specific energy (Equation 2.9), mechanical efficiency (Equation 2.10), and the bit-specific coefficient of sliding friction (Equation 2.11) as key indexes of drilling performance, the method makes bit selection and diagnoses different drilling operation situations.

$$E_S = \frac{WOB}{Borehole\ Area} + \frac{120\pi * RPM * Torque}{(Borehole\ Area * ROP)} \tag{2.9}$$

$$EFF_M = \frac{E_{s\,min}}{E_s} * 100 \tag{2.10}$$

$$\mu = 36 \frac{\text{Torque}}{(Bit\ Diameter * WOB)} \tag{2.11}$$

The authors define specific energy as the work done per unit volume of rock drilled. It assumes that the minimum specific energy required to drill is roughly equal to the compressive strength, σ, of the rock being drilled.

$$E_{S\,min} \approx \sigma$$

Therefore, the energy efficiency of drilling, $EFFM$, can be estimated by comparing the actual specific energy required to drill an interval with the minimum expected to be needed to drill that interval, EFF_{SMmin} or in Equation 2.10. The research analyzes the values of these three parameters in different rock types against RoP under different

situations, such as under atmospheric and hydrostatic pressure, different bits, different WoB and RPM, and different hydraulics. The following interpretations of drilling data are concluded:

1. Detection and correction of major drilling problems,
2. Analysis and optimization of drilling practices,
3. Bit selection,
4. Failure analysis,
5. Evaluation of new drilling technologies and tools,
6. Real-time monitoring and controlling of the drilling process,
7. Analysis of MWD data, and
8. Further development of expert systems.

2.3.3 John Rogers Smith, 1998-2000 [21, 22]

These research studies investigated poor bit performance in deep shale formations, and the focus of the study was to identify the characteristic symptoms of the problem for subsequent comparison to the symptoms resulting from different possible causes in laboratory tests. It used two measures for quantifying bit performance: mechanical-specific energy (Equations 2.12 and 2.13) and force ratio (Equations 2.14 and 2.15). Mechanical-specific energy is mechanical work being done at the bit per unit volume of rock removed. The force ratio is the ratio of the force acting to push the bit tooth or cutter laterally through the rock to break and remove it divided by the force acting downward to engage the tooth or cutter in the rock. It is similar to the dimensionless torque and coefficient of friction in the previous references. As observed in shale, if bit performance

decreases due to a balled bit, the force ratio is going to decrease, and specific energy is going to increase.

For full-scale test and field data:

$$E_S = \frac{WOB}{Borehole\ Area} + \frac{120\pi * RPM * Torque}{(Borehole\ Area * ROP)} \tag{2.12}$$

For single-cutter tests:

$$E_S = \frac{Axial\ Force}{\pi(Diameter\ of\ Path)(width\ of\ PDC)} + \frac{Tangential\ Force}{(Depth\ of\ cut\ (width\ of\ PDC))} \tag{2.13}$$

For full-scale test and field data:

$$R_f = 48\frac{Torque}{(Bit\ Diameter * WOB)} \tag{2.14}$$

For single-cutter tests:

$$R_f = \frac{Tangential\ Force}{(Axial\ Force)} \tag{2.15}$$

2.3.4 Charles H. King et al., 2000-2001 [24]

King et al. use a method of and system for optimizing bit rate of penetration while drilling by applying some special kind of linear regression as shown in Equation 2.16 on the weight of the bit and the rate of penetration to continuously determine an optimum

WoB as calculated by Equation 2.17, based upon measured conditions. The optimum WoB is maintained at the optimum level during relatively constant formation characteristics. As measured conditions change during drilling, the method updates the determinations of optimum WoB.

$$RoP = \alpha + \beta_1 RoP_{t-1} + \beta_2 RoP_{t-2} + \beta_3 WoB_t \quad (2.16)$$

$$WoB = \frac{RoP(1-\beta_1-\beta_2)-\alpha_k}{\beta_3} \quad (2.17)$$

2.4 Prior Work

The most common method of drilling oil wells consists of rotating a cutting bit, comprising individual cone bits, which is attached at the bottom of a hollow drill string of pipe and drill collars to progressively chip away the layers of earth. To force the chips of rock and earth formation to the surface, the common practice has been to force a fluid known as "drilling mud " or "drilling fluid" down the hollow drill string, thence outwardly between the cutting teeth to clear the teeth of accumulated dirt, and thence out into the annulus formed between the wall of the well which is being drilled and the exterior of the drill string. The mud picks up the chips of rock and earth and carries them with it to the surface, in this way to clear the well as it is drilled progressively deeper.

A typical cutter layout comprises three conical cutters of a rolling cone drill bit. The cutters are located in non-planar relationship. Typically tilted inward or outward. Each cutter comprises a generally conical body upon which are circumferentially located raised insert lands arranged circumferentially around the conical surface of cutter. Hard metal

cutting elements, commonly termed “inserts”, are located in cylindrical bores drilled into the cones perpendicular to the surface of lands.

Mud, as it is called, has a number of desired properties. It has a high viscosity and high density which makes it capable of carrying the cuttings from the rotating cutting bit up the annulus to the surface at a relatively low velocity, that is to say, about 125 to 150 feet per minute [5]. Should mud circulation be temporarily stopped, the settling velocity of cuttings is reduced. By reason of its high density, the mud tends to buoy up the drill string thereby to reduce the strain on the drilling rig, and mud in the annulus is at a high hydrostatic pressure which is exerted outwardly against the wall of the well and this helps prevent cave-ins and blow-outs which might occur as the result of high formation pressure. Additionally, finely divided solids suspended in the drilling mud work to build a filter cake on the wall of the well, frequently termed a bore hole, thus reducing loss of mud which might otherwise filter to the formation. The mud also serves to lubricate the bore hole wall. A further attribute of mud is that of lubricating the bearings of the cone bits, and keeping them relatively cool. The mud further serves as a medium, through which various types of logs are communicated to determine characteristics of the formations which have been penetrated as the drilling progresses.

In oil well drilling, directional bores (other than straight) are often drilled to recover oil from inaccessible locations; to stop blowouts; to sidetrack wells; to by-pass broken drill pipe; and for various other reasons.

Conventional techniques for directional drilling in wells use a deflector in the borehole to push the bit sideways (e.g. "whipstocking"); or alternatively insert a bent joint in the drilling string (e.g. "bent subs"); or alternatively propel pressurized drill mud sideways through a nozzle in the drill to push the bit sideways (e.g. "side jetting").

The "whipstocking" process requires a series of separate operations including drilling of a pilot hole, reaming of the pilot hole to full gauge, and removal of the deflector, and is therefore a time consuming and costly process. The use of "bent subs" to produce lateral forces on the drill bit requires the use of expensive drill motors; and the "side jetting" process, using special drill bits to provide offset holes by the pressurized drill mud, does not function well in hard rock earth since the conventional mud pressures will not erode the hard rock materials.

Various forms of earth boring bits are utilized to cut through the hard material formations in the earth when forming a well bore. One general form of drill bit utilizes one or more rolling cutters whose outer surfaces include projections such as milled teeth or cutter inserts that gouge into the formation material causing the material to disintegrate or pulverize as the cutter is rotated when the tool is turned about its axis. The rolling cutters are individually mounted to rotate about a supporting shaft or spindle typically with the axis of the spindle spaced radially from and at an incline with respect to the rotational axis of the tool. The incline of the spindle axis causes the cutter to both rotate about its axis and roll relative to the bottom of a borehole as the bit body is rotated. As a result, the cutter disintegrates a concentric ring of formation material in the bottom of the borehole.

One earlier version of the foregoing general type of rolling cutter is disclosed in U.S. Pat. No. 3,389,760 [26]. The patent discloses a rolling cone cutter supported to rotate upon a load pin which is connected at its opposite ends to a generally U-shaped support saddle. As disclosed, a number of such saddle and rolling cutter arrangements may be mounted on a single bit body for drilling a large borehole. For disintegrating formation, a multiplicity of small inserts of cemented tungsten carbide are fitted into drilled holes in each cutter body. The inserts are disposed in overlapping rows so that as the cutter is rolled over the bottom of a hole the inserts cut overlapping tracks so as to disintegrate the formation over the full width of a concentric swath defined by the length of the cutter as it is rotated around the axis of the drill bit.

The cutting elements of U.S. Pat. No. 3,389,760 [27] are in somewhat of a semi-random pattern on a smooth outer surface of the cutter. This physical arrangement of cutting elements leaves certain lateral discontinuities in the bottom hole pattern. As a result, the non-uniform succession of cutting elements often imparts an abrupt impact force during rotation of the cutter. Moreover, by design the outer surface of the cutter does not have relief grooves which initially aid in carrying away a disintegrated formation with the drilling fluid.

Ruhle, US3692125, 1972, [28] described a combination drilling and stimulation process for drilling oil wells, He described a drilling head in which the driiling mud flows outside the drilling string, which the mud carrying rock chips flows inside the inner pipe. The drill cones are so arranged for better clearing of the rock chips. However he recommends the use of a clear solution containing calcium chloride instead of the usual drilling mud. The solution of calcium chloride is treated with a liquified surfactant, and the mixture is

forced down the annulus formed between the drill pipe and drill collars, and the wall of the drill hole. At the bottom of the well the solution passes the cutting face of the bit and picks up the chips, flushing them outwardly through the drill collars and drill pipe and out at the top. The arrangement is aimed at the traditional vertical drilling only, and did not include any means for directional drilling.

Jones, US4420050, 1983, [29] An oil well drilling bit is disclosed of the type utilizing hard metal inserts in the rolling cutters wherein each row of inserts on each cutter is located thereon in a sinusoidal or varying pattern rather than the strictly circumferential pattern of the prior art.

Dardick,US4582147, 1986, [30] proposed a system for directional drilling of boreholes into the earth under control of the driller at the surface, employing a rotating earth drill including a projectile firing mechanism, that is timed to non-symmetrically repetitively fire repeatedly projectiles into the earth at controlled angular positions that are offset from the axis of the drill and drill string in the desired direction of drilling, as the drill progresses into the earth, thereby to fracture and break the rock in a desired direction other than straight ahead. The advancement of the rotary drill into the bore therefore follows a controlled path in the direction desired.

To remotely control the drill to fire the projectiles at a desired offset position or location as the bit rotates, the angle of rotation of the drill string is monitored at the surface, and the firing of the projectiles is remotely controlled from the surface to be "timed" to occur when the firing mechanism is rotatively positioned at a desired angle.

Wu, US 5230386, 1993, [31] (reissued Re 35,386 12/1996), describes a method for detecting and sensing boundaries between strata in a formation during directional drilling so that the drilling operation can be adjusted to maintain the drill string within a selected stratum is presented. The method comprises the initial drilling of an offset well from which resistivity of the formation with depth is determined. This resistivity information is then modeled to provide a modeled log indicative of the response of a resistivity tool within a selected stratum in a substantially horizontal direction. A directional (e.g., horizontal) well is thereafter drilled wherein resistivity is logged in real time and compared to that of the modeled horizontal resistivity to determine the location of the drill string and thereby the borehole in the substantially horizontal stratum. From this, the direction of drilling can be corrected or adjusted so that the borehole is maintained within the desired stratum.

Thompson, US5425429, 1995, [32] proposes a method for forming lateral boreholes from within an existing elongated shaft. A drilling unit is positioned within the existing shaft, bracing the drilling unit against a wall surrounding the existing shaft to transmit forces between the drilling unit and the medium surrounding the wall, and applying a drilling force from the drilling unit to cut through the wall of the existing shaft and form the substantially lateral borehole in the surrounding medium. The method includes an extendable insert ram within the drilling unit for extending a drill bit from the drilling unit and applying a drilling force to the drill bit to cut through the wall of the existing shaft. A supply of modular drill string elements are cyclically inserted between the insert ram and the drill bit so that repeated extensions of the insert ram further extends the drill bit into the surrounding medium to increase the length of the lateral borehole. The

method has no provision for true directional steering and is not suitable for oil drilling, as the extensions of the lateral drilling string is limited by collars that can only fit within the main hole.

Saxman, US5429201, 1995, [33] Presented an improved bit design in which the drill bit includes a rolling cutter having a plurality of circumferential rows of teeth protruding from the body of the cutter. At least one of the rows of teeth is a closed-end circumferential row located on the surface of the cutter along a closed-end circumferential path. The latter is a non-circular curve defined by a surface intersecting the body of the cutter obliquely with respect to its longitudinal axis.

Gipson, US 5439066, 1995, [34] described a method and system for translating the orientation of a length of coil tubing from a generally vertical orientation to a generally horizontal orientation, inside a well borehole and downhole of a wellhead. A first conduit is installed and suspended in a well borehole. The conduit is provided with a coil tubing bender at the downhole end of the conduit. Coil tubing is injected into the conduit through an upper packer attached to the top section of the conduit. After a section of coil tubing is injected into the conduit, an outer coil tubing seal is securely affixed to the coil tubing. The coil tubing is run to the top of the bender; the packer is closed; and high pressure fluid is introduced between the upper packer and the outer seal inside the conduit. The fluid forces the coil tubing through the bender and translates the coil tubing from a vertical to horizontal orientation. Abrasive fluid may be pumped at high pressures through the coil tubing now in the horizontal orientation, thereby creating a horizontal bore in the formation.

Hathaway, US 5553680, 1996 [35] disclosed a horizontal boring apparatus which is comprised of a remotely controlled drilling tool lowered from a self-contained vehicle into a previously drilled vertical shaft. The tool mills away a 360 degree band of metal casing adjacent to the desired area to be bored, and extends a hydraulic powered rotary drilling tool into the formation by extending and retracting a telescoping base while alternating stabilization of the base and bit end of the drilling tool much like an inch worm. The tool is designed to drill a 1 inch bore hole up to 150 feet in any direction, or several directions. The tool and tool housing contain instrumentation for sensing direction, inclination, density, and temperature.

Kuenzi, US 6308789, 2001, [36] described a drill bit that is arranged to change the direction of drilling. A cone head is rotatably mounted on a shank portion extending from an elongate housing. When the housing is rotated, the cone head generates a concave hole. When a change in direction is required, the housing is rotated a few degrees in one direction and then counter-rotated in the opposite direction. This generates a partial but redirected pilot hole that is also substantially concave in configuration. Continued full rotation causes the drill bit to follow the partial pilot hole in the new direction.

Haci et al., US 6802378, 2004, [37] described a method of and system for directional drilling reduces the friction between the drill string and the well bore. A downhole drilling motor is connected to the surface by a drill string. The drilling motor is oriented at a selected tool face angle. The drill string is rotated at said surface location in a first direction until a first torque magnitude without changing the tool face angle. The drill string is then rotated in the opposite direction until a second torque magnitude is reached,

again without changing the tool face angle. The drill string is rocked back and forth between the first and second torque magnitudes.

Sved, US 6810971, 2004, [38] described various steerable horizontal subterranean drill bit apparatuses, which may have a drill bit, a housing and a one-bolt attachment system, or other features.

Adam et al, US 7195082, 2007, [39] disclosed a method of steering a fluid drilling head in an underground borehole drilling situation is provided by rotating the flexible hose through which high pressure is provided to the drilling head and providing a biasing force on the drilling head. The hose can be rotated from a remote surface mounted situation by rotating the entire surface rig in a horizontal plane about a turntable causing the vertically orientated portion of the hose to rotate about its longitudinal axis. The biasing force can be provided in a number of different ways but typically results from the use of an asymmetrical gauging ring on the fluid drilling head.

Russell , US 7543658, 2009, [40] described a drilling means for directional drilling in a bore hole comprising a drill pipe and a drilling head, including a slippable clutch device linking the drill pipe and said drilling head such that torque due to rotation of said drill pipe can be controllably applied to said drilling head through at least partial engagement of said clutch, and control means operable to sense an actual orientation angle of said drilling head and compare said actual orientation angle with a required orientation angle adjustably set in said control means and to control said slippable clutch such that when the actual orientation angle and the required orientation angle are the same, the slip

torque of the slipping clutch equals the motor reaction torque, so maintaining the orientation angle of the drilling tool at said required orientation angle.

Al Hadhrami, US 7958949, 2011, [41] described a technique for drilling a borehole includes obtaining data from a tool in the borehole for a plurality of positions in the borehole that is being drilled to form acquired data indicative of directional electromagnetic propagation measurements. The technique includes identifying a plurality of distances to a boundary between formations in ground from the plurality of positions in the borehole based on the measurements; identifying a trajectory of the borehole using the plurality of distances; and deciding whether to change the trajectory of the borehole using a change in the plurality of distances between the trajectory and the boundary. The trajectory of the borehole may be changed in both inclination and azimuth.

CHAPTER 3

MODELING OF DIRECTIONAL STEERING SYSTEM

3.1 Introduction

A Directional Steering System (DSS) equipped with four motors (5), shown in Figure 3.1 with each a drill bit attached. The speed of the each motor can be independently controlled, causing the rate of removal of rocks by each bit and the direction of advancement of the drilling head to be precisely controlled. The drill head assembly is attached to the end of the drill string (2), which includes an inner pipe for carrying the drilling fluid. The use of four motors in coordination with other traditional drilling variables allow precise control of the drilling direction and optimization of Rate of Penetration (RoP).The top and bottom motors rotate clockwise direction while the right and left motors rotate counter clockwise direction. Pitch movement (inclination) is obtained by increasing or decreasing the speed of the top motor while decreasing or increasing the speed of the lower motor. The yaw movement (azimuth) is obtained similarly using the right and left motors. The control of the four motors allow better management of the drilling operation in various drilling environment and under various operational constraints.

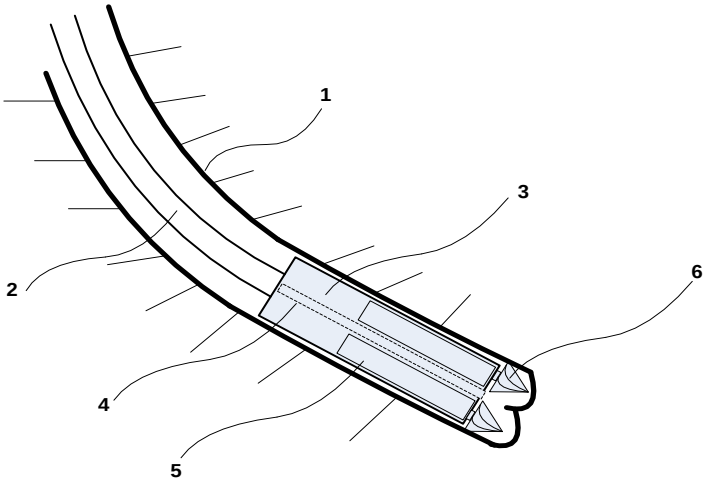

Figure 3.1: Overview of the drilling assembly

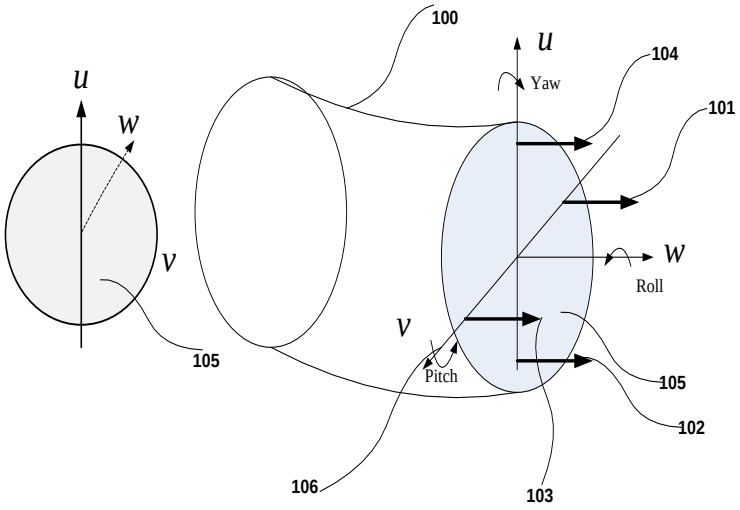

Figure 3.2: Reference axis for the drilling assembly

According to one embodiment, shown in Figure 3.2, (100) is the hole bore. The 4 drill bits are arranged symmetrical with respect to three body axes {U,V,W} (106), where the W-axes is coming out of the page in the direction of motion. The tool face (105) is taken to be the {U,V} plane. The right motor thrust is (103), the left motor thrust is (101), the top thrust is (104), and the bottom thrust is (102). Rotors (101) and (102) rotate CCW,

while rotors (103) and (104) rotate CW. The rotors could be electrical motors or hydraulic mud motors with power control, and torque/rpm sensors. The directions of the body yaw (azimuth), roll and pitch (inclination) are also indicated in Figure 3.2.

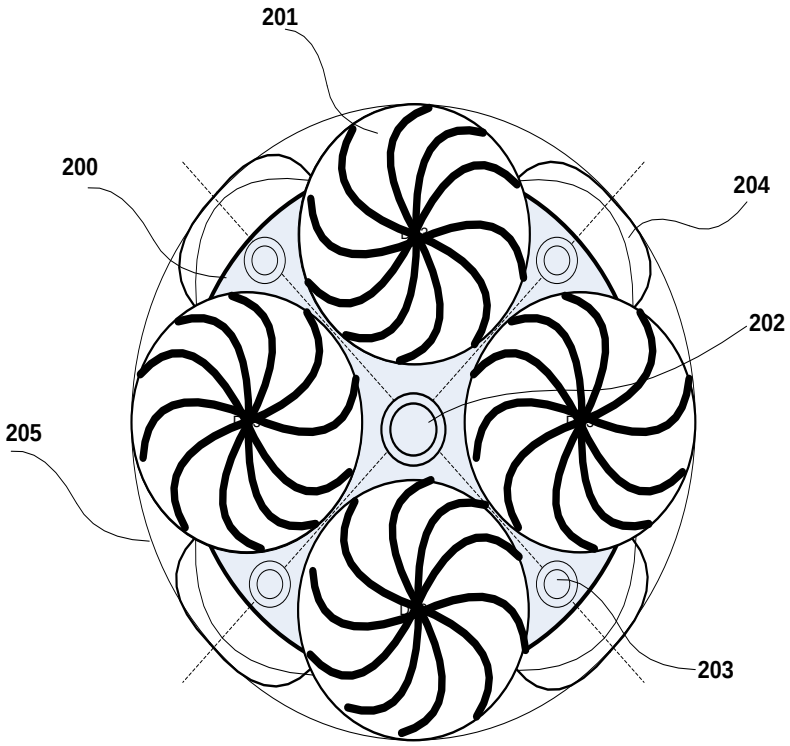

Figure 3.3: The drilling assemble front projection

Figure 3.3, depicts the a schematic of the BHA as projected towards the tool face. (200) is the BHA cylindrical casing, and (205) is the bore hall. (202) is the central nozzle for ejecting the drilling fluid (mud), (203) are four side nozzles for removal of circumferential rock chips, (204) front chisels fixed to the drill body for crushing circumferential debris and smoothing the surface of the borehole. (201) are four conic drill bits with twisted blades for crushing and removal of the rocks.

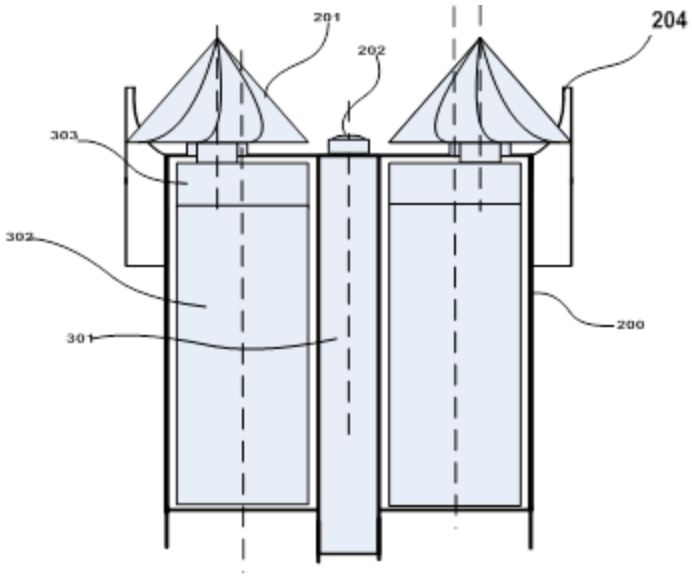

Figure 3.4: Side cross section of the drilling assembly

Figure 3.4 depicts a longitudinal cross section view of the drilling head assembly showing two motors (out of four) (302). A body (200), the central nozzle (202), a central pipe (301) for carrying the inlet mud fluid. The figure also shows two drill bits (out of four) (201) connected to the motors via a gear box (303). The chisels (204) help to crush rocks and smooth out the circumference of the bore hole. The drilling fluid can be made to be in contact with motors heat sinks to cool the motors.

The BHA, Figure 3.5, may include a section for conventional Measurements while drilling MWD (504), and another section for conventional log while drilling (LWD) (505), in addition to other instruments for measurement of body angular velocities and acceleration to track the orientation and position of the BHA. The MWD includes three perpendicular set of accelerometers for gravity measurements to determine the vertical axis, and three magnetometers for determining the magnetic north. The accelerometers and magnetometers are aligned with the BHA body axis, The BHA may also include a

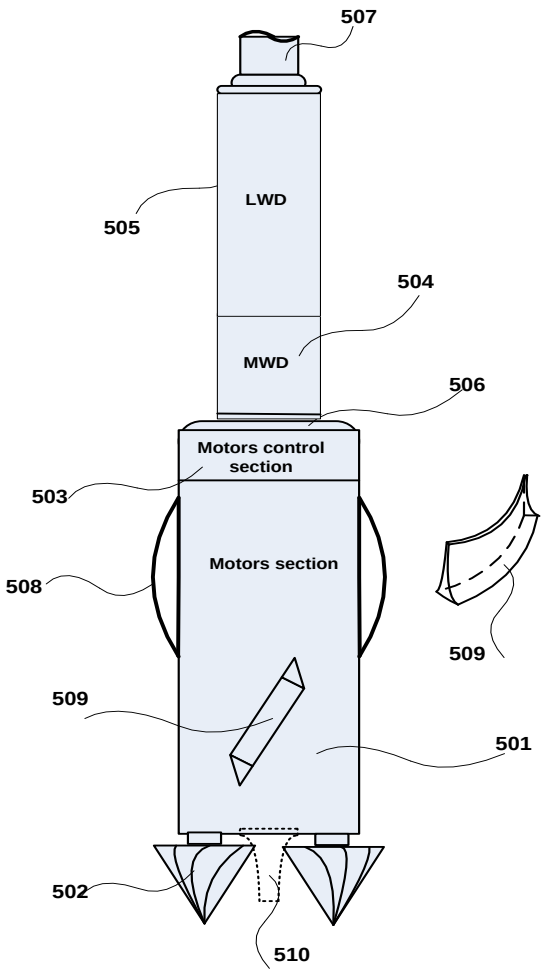

Figure 3.5: Components of the BHA

hydraulic generator and other motor control electronics and actuators. Attached outside the drilling head plurality of sliding surfaces (508) along the longitudinal axis to reduce friction during horizontal drilling. The sliding surfaces could be housed inside the drilling head casing and brought out when needed. Attached out also outside the surface of the drilling head a plurality of smoothing surfaces (509) inclined to the longitudinal axis to smooth the borehole. Similarly, front chisels are also attached to drilling head to remove left over rock parts, which could be inaccessible by the four drilling bits.

In conventional oil drilling the bits are deigned to achieve the best rock crushing capability. The motor torque is utilized for rock crushing, while the task of moving the debris is performed by the mud fluid jet. Unlike the conventional drill bits, the invention discloses a new bit design, where the motor torque is converted by the bit structure to a drag torque T_D and a lift force F_L. The drag torque contributes to the crushing the rocks, while the lift force removes the debris and causes a forward thrust force on the BHA body.

Several designs can be used for the drill bits as shown in Figure 3.6. One of the unique design feature of the proposed drill bit is its twisted blades as depicted in Figure 3.6.

The bit design parameters are

Nb : number of blades

Vb: grove volume per blade

τ_b: twist angle

d1, d2, and L: drill dimensions (depend on the bore diameter and rock type).

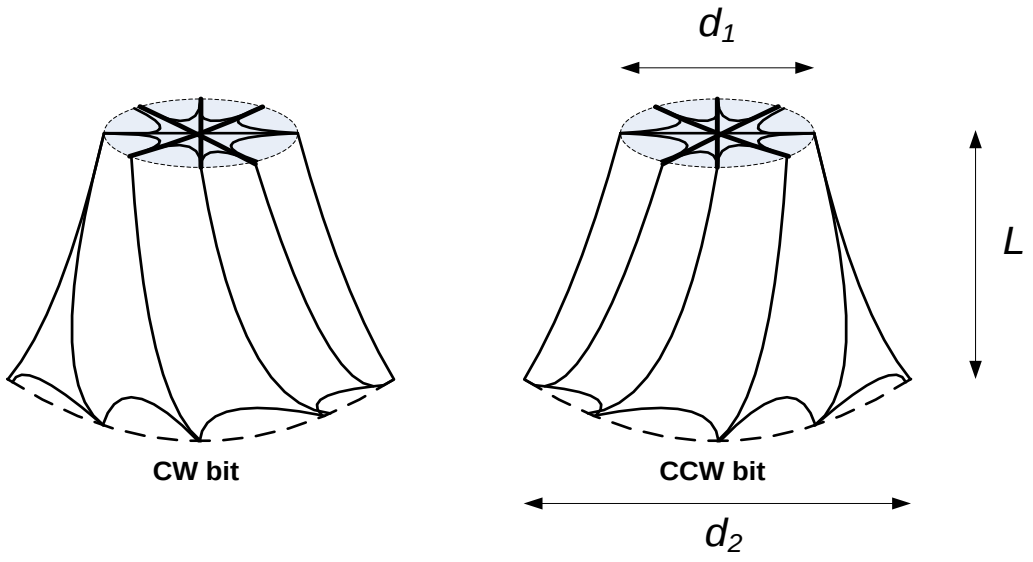

Figure 3.6: Design parameters of drill bit

Clearly other design features could be added to the basic design depending on the depth and rock type, for example using wavy blades, adding inserts, and diamond parts along the edges of the blades.

3.2 Drag Torque and Left Force

The motor torque is resolved by the drill bit into two components; a drag torque on a plane perpendicular to the bit axis (T_D), and a lift force (F_L), which moves crushed debris up through the bit helical groves. In effect, this lifting force will exert a forward thrust force on the drill head along the bit axis. The left force is approximated by the relation

$$F_L = b.w_i^2$$

where b is the thrust factor and ω is the angular speed of the bit. The coefficient b depends on the bit geometry and the density of mud. The second component of the bit effort is the drag torque, which is used to crush the rocks. The drag torque, T_D may be approximated by the relation

$$T_D = d\omega_i^2$$

Where, d depends on the drill bit geometry, rock density, and rock specific energy. The four rotational velocities w_i of the rotors are the input control variables, or equivalently, the motors power, P_i, i=1,2,3,4.

3.2.1 Specific Energy

As the drilling goes on, DSS drills the hole by crushing the rocks, for that it requires sufficient amount of forces and torques. For different surface layers it requires exact

amount of force to achieve smooth flow of operation and high productivity. Specific Energy principles provides a method of predicting performance of bit. It is a useful parameter which can be defined as work done by unit volume excavated [42]. The amount of rock excavated is measured geometrically by volume. It is evident that in order to crush the rock, a minimum quantity of energy is required. The amount of energy is entirely depends on the layers and the nature of rocks. The mechanical process during crushing the rocks might or might not approach the requirements, such as breaking the rocks in a smaller fragments than necessary. Friction between the tool and rocks, mechanical losses are the primary effects for getting the smaller fragments than required.This effect is illustrated by Walker and Shaw and he proposed [43] the idea of constant specific energy, which makes possible to achieve maximum mechanical efficiency. The mechanical efficiency of the rock cannot be measured directly. The volume of rock broken per unit energy input is reciprocal of specific energy, so that mechanical efficiency is a maximum when specific energy is a minimum.

3.2.2 Control Inputs

By using the Specific Energy(Es) Principles we developed two equations

1. The Left Force(F_L).
2. Drag Torque(T_D).

A drag torque on a plane perpendicular to the bit axis (T_{D}), and a left force (F_L), which moves crushed debris up through the bit helical groves. In effect, this left force will exert a forward thrust force on the drill head along the bit axis.

$$Q = V_b N_{bt} * rpm/60 \tag{3.1}$$

$$Q_M = Q + Q_F = Q(1 + \alpha_m) \tag{3.2}$$

therefore,

$$F_L = \rho_i A_b [gh + \frac{1}{2}\left(\frac{Q_m}{A_b}\right)^2] \tag{3.3}$$

The bit interaction with the formation can be described by a Left Force (F_L) and a Drag Torque (T_D). The F_L and T_D are related to the motor torque by the relationship

$$F_L = \propto_1 T_m, T_D = \propto_2 T_m$$

Where, T_m is the motor torque, and α_1, α_2 depend on the drill bit geometry. On the other hand, for a given power the motor torque-speed relationship is defined by the motor characteristic. The straight line (linear relation) in Figure 3.7 illustrates a simplified and normalized motor torque-speed characteristic curve. The curve moves up for increased motor power. The operating speed is determined by the balance between the motor torque-speed and the load torque-speed. The load torque-speed, illustrated by the dotted curve in Figure 3.7**,** depends on the formation characteristics and the operating parameters as fluid type and flow rate. At the operating speed (the intersection point of the two curves in Figure 3.7), the left force is the force required to move the material up by the drill bit.

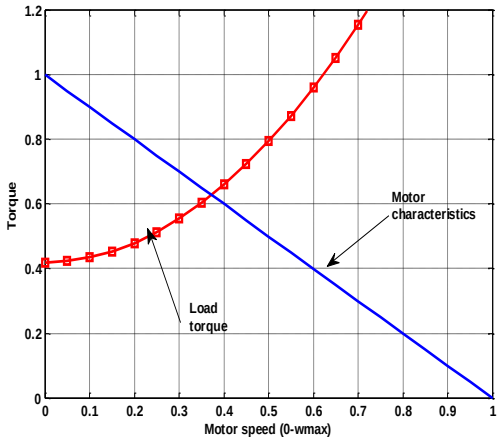

Figure 3.7: Characteristics of F_L and T_D $with$ T_m

The left force generated by each drill bit is given as $F_L = b\omega_i^2;\ i = 1,2,3,4.$

where

$A_b -$ cross section area of hole;

$V_b -$ chip volume per revolution per tooth;

$N_{bt} -$ number of teeth in the bit;

$D_b -$drill bit diameter ;

$Ei -$ specific energy of the ith formation $\frac{KJ}{kg}$;

$\rho_i -$ density of the ith formation ;

$Pi -$ compression strength of the ith formation, it is function of the rock composition, porosity, and depth (compactness) ;

$\alpha_m -$ volume flow rate of the injected fluid/rate of rock volume removal;

$Q -$ideal volume rate of rock removal;

$Q_F -$ rate of injected fluid;

$Q_M -$mud volume flow rate $\frac{m^3}{sec}$.

The second component of the bit effort is the drag torque, which is used to crush the rocks. The drag torque, $T_D$may be approximated by the relation $T_D = d\omega_i^2$, where d depends on the drill bit geometry, rock density, and rock specific energy.

The drag torque is the bit torque used to crush the rocks

Power of the drag torque;

$$T_D * 2\pi * \frac{rpm}{60} = V_b N_{bt} \rho_i E_i * rpm/60$$

The drag torque

$$T_D = \frac{V_b N_{bt} \rho_i E_i}{2\pi} \tag{3.4}$$

So. The drag Torque required by each drill bit is given as $T_{D_i} = d\omega_i^2$; $i = 1,2,3,4$.

The four rotational velocities w_i of the rotors are the input variables, but with regard to the obtained model a transformation of the inputs is suitable. We define the new inputs from (3) and (5) are:

$$u_1 = F_{L_1} + F_{L_2} + F_{L_3} + F_{L_4} \tag{3.5}$$

$$u_2 = F_{L_2} - F_{L_4} \tag{3.6}$$

$$u_3 = F_{L_1} - F_{L_3} \tag{3.7}$$

$$u_4 = T_{D_1} + T_{D_3} - T_{D_2} - T_{D_4} \tag{3.8}$$

Additionally, another control input is usually used to improve the rate of penetration called Force on Bit (FoB). FoB is a quantitative term used to express the amount of axial force placed on the drill bit assembly. This force directly acts on the center axis of a system. So we considered FoB as an additional part of input variable u_1 which provides additional compression force to break rocks, depending on direction. Therefore u_1 becomes:

$$u_1 = F_{L_1} + F_{L_2} + F_{L_3} + F_{L_4} + FoB. \tag{3.9}$$

In order to break the rock the Torque (T_D) of the rotors should be higher than the Left force (F_L) i.e $T_{D_i} \gg F_{L_i}$. However, higher values of F_L, are needed to improve steering and rate of penetration.

3.3 Rotating and Fixed Frames

When dealing with drilling objects it is convenient to be able to describe vectors not only in a global frame, but also in a rotating local body frame. This control room is defined to be the inertial frame from where the model will be described. The earth fixed inertial frame is from now referred to as the earth frame. The rotating frame following the attitude of the DSS is denoted the body frame. For this assumption to make sense the structure of the DSS is assumed to be rigid. That a body is rigid is defined such that the distance between any two points in the structure will always remain the same no matter how the body is positioned or oriented.

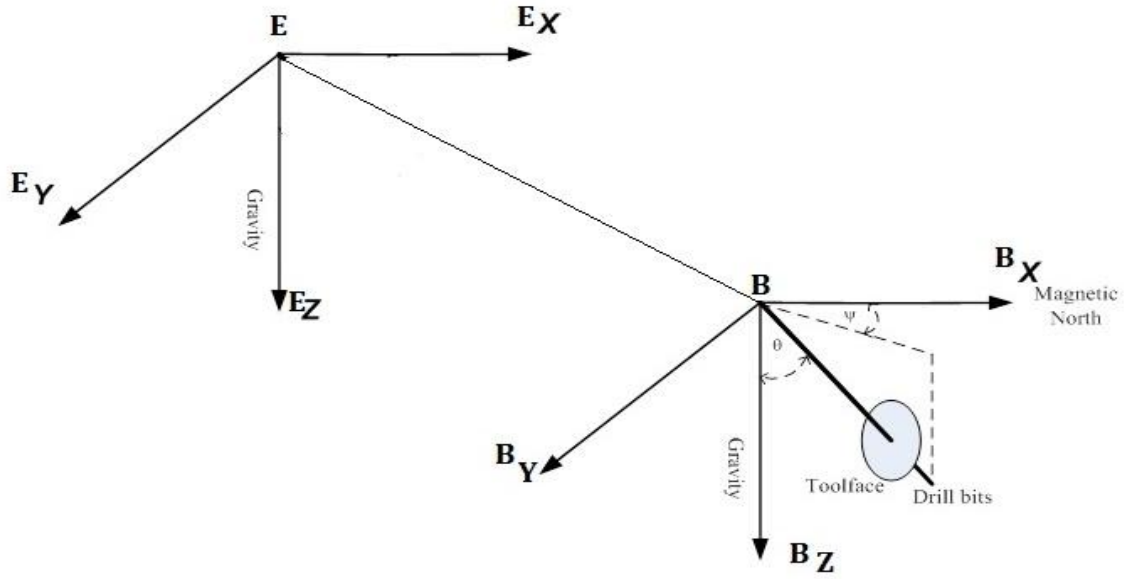

Figure.3.8: Earth and Body frame

Figure 3.8 shows the two frames. To the left the earth fixed frame denoted E and to the right the body fixed frame denoted B. When a vector is seen with respect to the earth fixed frame it will either be denoted with an e in front of the vector or nothing at all. Likewise if the vector is seen with respect to the body frame it will be denoted with b.

We are considering two frames : Inertial earth frame (observer from control room) and Body fixed frame. The position of the Drill bits in the inertial frame is given by the vector

$$\zeta^T = (x, y, z)$$

3.4 Orientation and Rotations

The orientation of the DSS will be described as a parameterization of the transformation from the earth frame to the body frame. In this thesis the Euler angle parameterization is used.

The Euler angles are widely used, since they have a very clear physical interpretation and are of minimum dimensionality. The minimum required dimensionality for describing an orientation in 3 dimensions is 3. However, the orientation cannot be both global and non-singular with less than 4 dimensions [29]. The parameterizing of the rotational matrix, using Euler angles, includes multiple trigonometric functions, which leaves the transformation non-linear and is subject to gimbal lock.

3.4.1 Euler Angles

The Euler angle parameterization utilizes that the orientation of one cartesian coordinate system, with respect to another, can always be described by three successive rotations. The orientation of a coordinate system can therefore be described by the z,y,x (also called 3-2-1) right-hand rotation sequence that is required to get from earth frame into alignment with the body frame. Other sequences can be used as well, but the 3-2-1 sequence is used when dealing with DSS.

The orientation of the 4-Motor drill bit's system is given by the three Euler angles, namely yaw angle ψ,Pitch angle θ and the roll angle ϕ .that together form the vector

$$\Omega^T = (\phi, \theta, \psi)$$

We assume initially, the body axis UVW were aligned with the inertia axis XYZ. The body is subject to rotation ψ about the Z-axis, followed by θ about V-axis (pitch), followed by a roll rotation φ about the W axis.

Accordingly, the sequence of transformation can be expresses as

$$R_{BE} = R_{U,\psi} R_{V,\theta} R_{W,\phi}$$

$$R_{BE} = \begin{bmatrix} c\psi & -s\psi & 0 \\ s\psi & c\psi & 0 \\ 0 & 0 & 1 \end{bmatrix} \begin{bmatrix} c\theta & 0 & s\theta \\ 0 & 1 & 0 \\ -s\theta & 0 & c\theta \end{bmatrix} \begin{bmatrix} c\phi & -s\phi & 0 \\ s\phi & c\phi & 0 \\ 0 & 0 & 1 \end{bmatrix}$$

$$R_{BE} = \begin{bmatrix} c\psi c\theta c\phi - s\psi s\phi & -c\psi c\theta s\psi - s\psi c\phi & c\psi s\theta \\ s\psi c\theta c\phi + c\psi s\phi & -s\psi c\theta s\phi + c\psi c\phi & s\psi s\theta \\ -s\theta c\phi & s\theta s\phi & c\theta \end{bmatrix} \quad (3.10)$$

The rotational matrix R_{BE} defines the transformation from the body axis to the inertia axes, for a point P in space, where $c\theta$ denotes $\cos\theta$ and $s\theta$ denotes $sin\ \theta$.

$$P_{XYZ} = R_{BE} P_{UVW}$$

The inverse transformation matrix Q is given by

$$Q = R_{BE}^{-1} = R_{BE}^{T}$$

$$R_{BE}^{T} = \begin{bmatrix} c\psi c\theta c\phi - s\psi s\phi & s\psi c\theta c\phi + c\psi s\phi & -s\theta c\phi \\ -c\psi c\theta s\psi - s\psi c\phi & -s\psi c\theta s\phi + c\psi c\phi & s\theta s\phi \\ c\psi s\theta & s\psi s\theta & c\theta \end{bmatrix}$$

and R_r is the rotation Matrix,

$$R_r = \begin{bmatrix} c\psi & -s\psi & 0 \\ s\psi & c\psi & 0 \\ 0 & 0 & 1 \end{bmatrix}$$

$$P_{UVW} = Q P_{XYZ}$$

3.5 Forces and Torques

Vector $\zeta = [x\ y\ z\ ]^T$ describe the posisiton of the center of gravity in Earth Frame and the three independent angles $\eta = [\phi\ \theta\ \psi]^T$, respectively roll, pitch and yaw ,which describe the DSS orientation.

Also $V = [u\ v\ w\ ]^T\ and\ \Omega = [p\ q\ r\ ]^T$ are the translational velocity vector and the rotation velocity vector in the body frame.

Therefore,

$$\dot{\zeta} = R_{BE}V \tag{3.11}$$

$$\Omega = R_r\dot{\eta} \tag{3.12}$$

By differentiating the above equations 3.11and 3.12 we obtain,

$$\ddot{\zeta}\ = R_{BE}(\dot{V} + \Omega \times V) \tag{3.13}$$

$$\dot{\Omega} = R_r\ddot{\eta} + ((\partial R_r/\partial\theta)\dot{\theta} + \left(\frac{\partial R_r}{\partial\psi}\right)\dot{\psi})\dot{\eta} \tag{3.14}$$

By newton's law the forces acting on the DSS is given by

$$F_{ext} = m\dot{V} + \Omega \times (mV) \tag{3.15}$$

$$T_{ext} = J\dot{\Omega} + \Omega \times (J\Omega) \tag{3.16}$$

Where $m\ and\ J$ are the mass and the total Inertia matrix of the DSS.

$$J = \begin{bmatrix} I_x & 0 & 0 \\ 0 & I_y & 0 \\ 0 & 0 & I_z \end{bmatrix}$$

The main force apart from F applying to the DSS is the gravitational force.The gravitational force is always pointed down in the earth fixed frame and can be described as in Equation 3.17

$$\begin{bmatrix} g_x \\ g_y \\ g_z \end{bmatrix} = Q \begin{bmatrix} 0 \\ 0 \\ 1 \end{bmatrix} = \begin{bmatrix} -s\theta \\ s\theta s\phi \\ c\theta \end{bmatrix} \tag{3.17}$$

The three relations defined in Equation 3.17 can be used to find the actual attitude of the BHA,$(\psi_A, \theta_A, \phi_A)$. Similar equation can be derived based on the known direction of magnetic north and the measurements of magnetometers in the MWD unit.

The components of the gravitational force in the body $U\&V$ directions are given by

$$f_{gu} = -s\theta c\phi mg$$

$$f_{gv} = s\theta s\phi mg$$

Since the motion is confined to the borehole, these two components do not cause lateral movements and are cancelled by formation reaction forces. However, these two components determine the friction forces in the direction of motion and the friction torque against angular motion around w-axis as follows

$$F_{fw} = \mu * (s\theta c\phi mg + s\theta s\phi mg) \tag{3.18}$$

Where μ is the friction coefficient (0.25 ~0.4).

During vertical drilling ($\phi = 0$) the friction force is negligible, while in the horizontal drilling the friction force is maximum.

The friction torque is given by

$$T_{fw,\psi} = \mu * Cos\theta.(s\theta c\phi mg + s\theta s\phi mg) \tag{3.19}$$

The gravitational direction is measured in the Measuring While drilling (MWD) unit by three accelerometers aligned along the body axis. The Gravitational direction can be expressed in of the normalized accelerometer reading as

$$F_{grav} = mgcos\theta$$

The total sum for forces $F_{ext}$and torques T_{ext} described as:

$$F_{ext} = F - F_{grav} \tag{3.20}$$

$$T_{ext} = T - T_G - T_f \tag{3.21}$$

Where $F\ and\ T$ are the Forces and Torques given to the DSS as the control inputs, F_{grav} , T_G and T_f are the gravitational reaction force, gyroscopic torque and friction torque acting on a DSS.

The forces and Torques are given as:

$$F = \begin{bmatrix} 0 \\ 0 \\ u_1 \end{bmatrix}; T = \begin{bmatrix} u_2 \\ u_3 \\ u_4 \end{bmatrix}$$

Finally using above equations $3.11 - 3.22$, we obtained the dynamics of DSS as follows:

$$m\ddot{w} = \left(u_1 - F_{fw}\right) + mgcos\theta \tag{3.23}$$

Similarly the Torques T will become as

$$T = \begin{bmatrix} L_b u_2 \\ L_b u_3 \\ L_b u_4 \end{bmatrix}; \qquad T_f = \begin{bmatrix} 0 \\ 0 \\ T_{fw} \end{bmatrix};$$

$T_G = I_r \left(\dot{\eta} \times \begin{bmatrix} 0 \\ 0 \\ 1 \end{bmatrix} \right) . (RPM_1 - RPM_2 + RPM_3 - RPM_4) * 2 * \frac{\pi}{60}$, in Inertial frame.

Now substituting the above equations of T_{ext}, T, T_G in equation 3.21 we get;

$$J\dot{\Omega} + \Omega \times (J\Omega) = \begin{bmatrix} L_b u_2 \\ L_b u_3 \\ L_b u_4 \end{bmatrix} - T_G - T_f$$

$$\ddot{\psi} = \dot{\theta}\dot{\phi}\left(\frac{I_y - I_z}{I_x}\right) - \frac{I_r}{I_x}\dot{\theta} g_y + \frac{L_b u_2}{I_x} \tag{3.24}$$

$$\ddot{\theta} = \dot{\phi}\dot{\psi}\left(\frac{I_z - I_x}{I_y}\right) + \frac{I_r}{I_y}\dot{\psi} g_y + \frac{L_b u_3}{I_y} \tag{3.25}$$

$$\ddot{\phi} = \dot{\theta}\dot{\psi}\left(\frac{I_x - I_y}{I_z}\right) + \frac{L_b u_4}{I_z} - T_{fw,\psi} \tag{3.26}$$

where, I_r is inertia of the drill bit and

$$g_y = (RPM_1 - RPM_2 + RPM_3 - RPM_4) * 2 * \frac{\pi}{60}$$

The structure of the model is shown in Figure 3.9

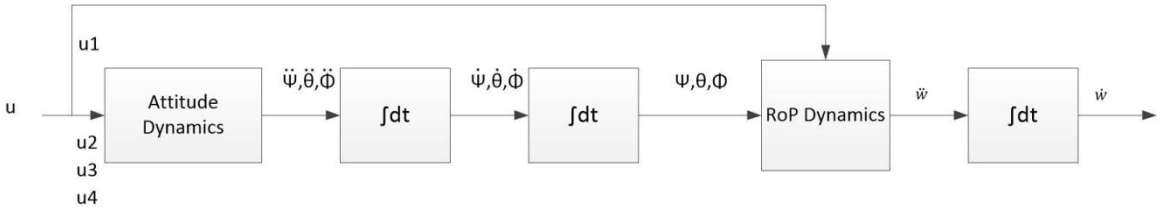

Figure.3.9: Structure of a DSS Model

3.6 Simulations

The derived dynamic model has been implemented in Matlab/Simulink and the parameters required for the simulation is given in TABLE 3.1

TABLE 3.1 Parameters of DSS

Parameter	Value	Unit
g	9.81	m/s^2
m	200	Kg
D	$18-24$	$inches$
L	0.55	m
$I_{xx}=I_{yy}$	60	Kg/m^2
I_{zz}	25	Kg/m^2
I_R	0.83	Kg/m^2

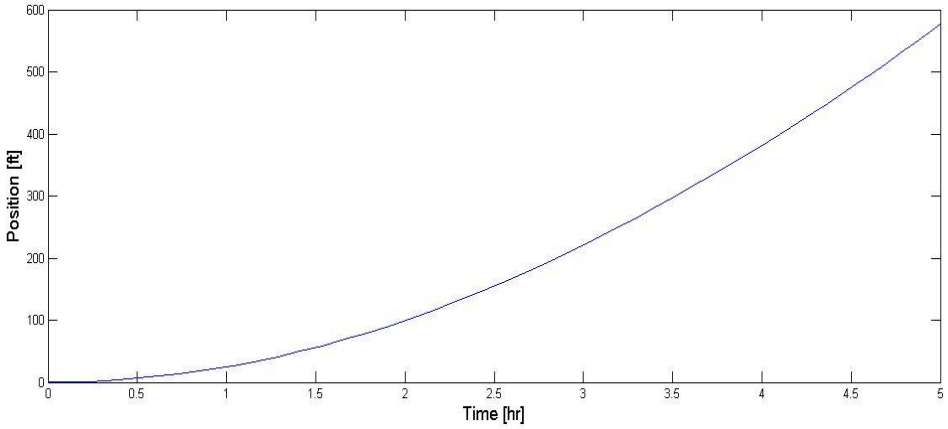

Figure 3.10: Position

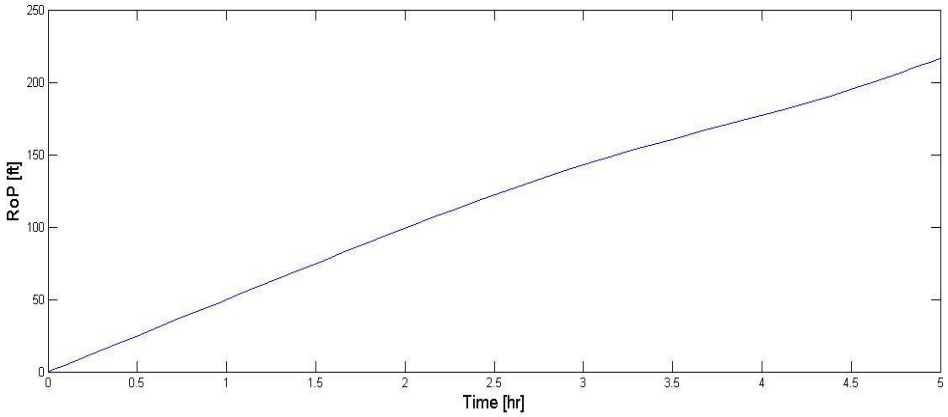

Figure 3.11: RoP

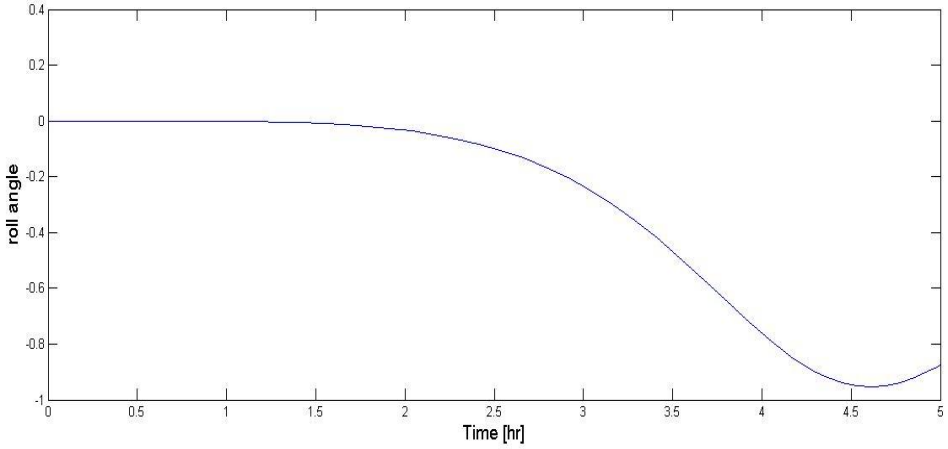

Figure 3.12: Roll angle ϕ

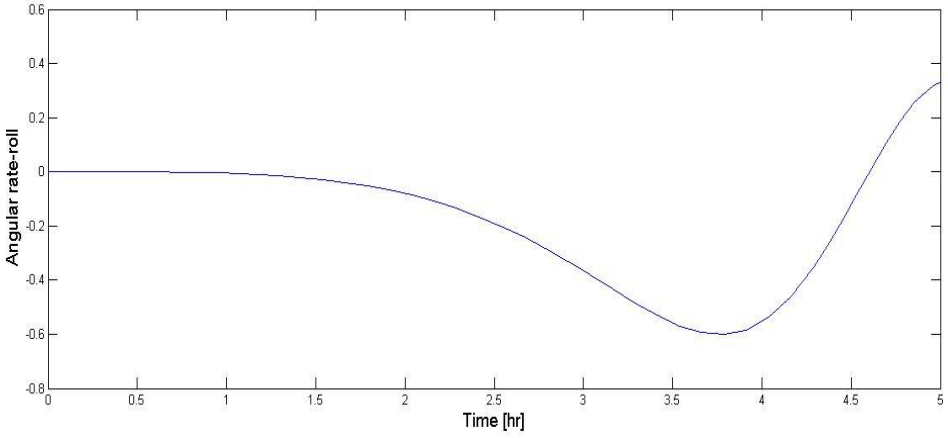

Figure 3.13: Pitch angle θ (inclination)

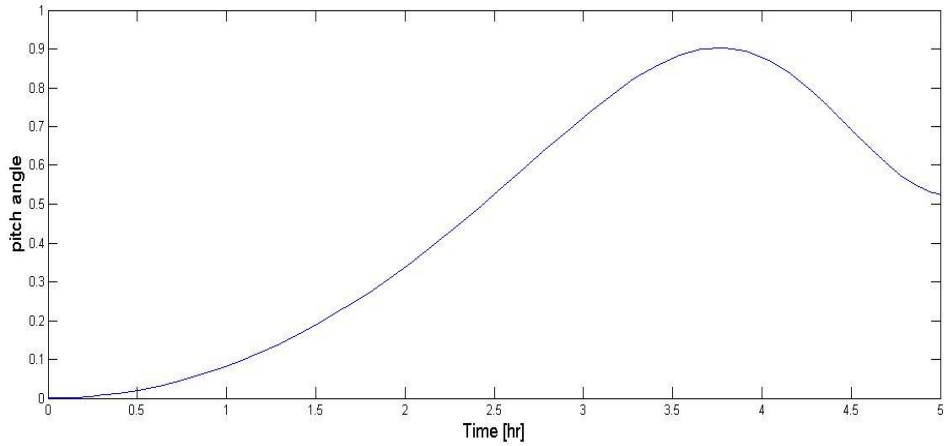

Figure 3.14: Yaw angle ψ (azimuth)

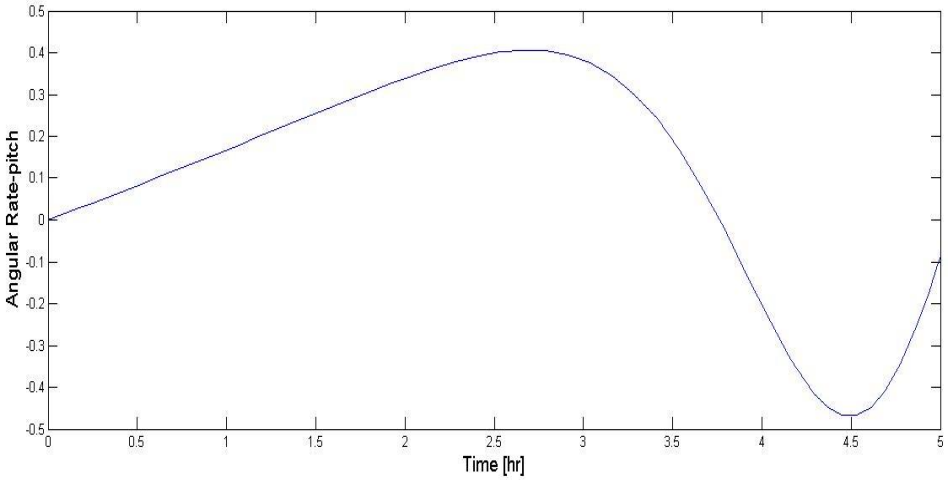

Figure 3.15: Angular rate-pitch $\dot{\theta}$

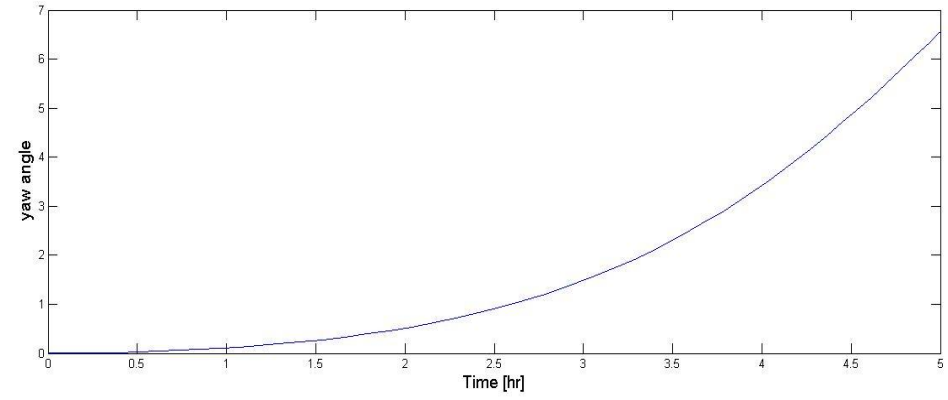

Figure 3.16: Angular rate-roll $\dot{\phi}$

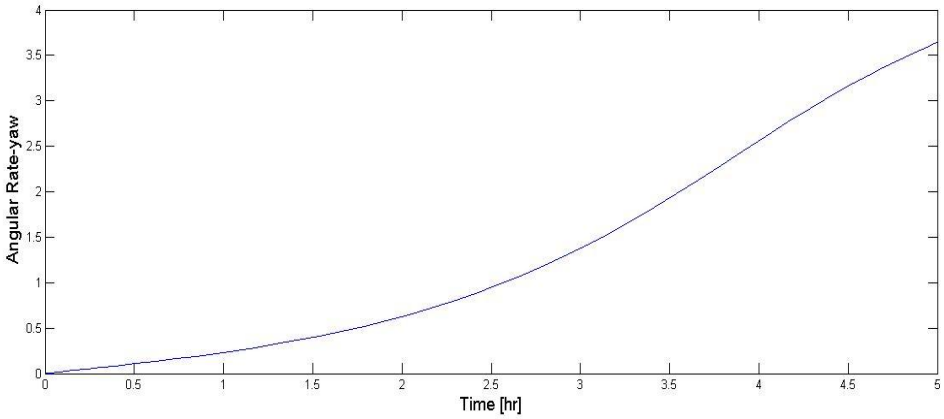

Figure 3.17: Angular rate-pitch $\dot{\psi}$

CHAPTER 4

CONTROLLER DESIGN

4.1 Introduction

The presented model in the previous chapter serves as the basis for the development of the control system. The tasks of the control system involve very high speed motions and the non- linear effects will be significant in the dynamics and the non-linear controller is required to achieve the desired performance.

Four control loops are involved in the control of steering, as follows:

The Attitude controller level consists of the three loops: inclination, azimuth and roll stabilization and the another level is of RoP controller. In Inclination control loop, where the difference between the desired and actual inclination is used to adjust the auxiliary input variable u_3. The Azimuth control loop, where the difference between the desired and actual azimuth angles is used to determine the auxiliary variable u_2. The roll stabilization loop, where the roll offset is used to determine the auxiliary variable u_4.

The RoP control loop, where the difference between the desired RoP and the actual RoP is used to determine the auxiliary input variables u_1. The loop is also affected by FoB, as usually the motors are not enough to achieve the required rock crushing rate.

The desired RoP is determined by an outer optimization algorithm, which includes tool wear rate, motors power constrains, formation properties, mud fluid properties, flow rate, and hydraulic power.

The auxiliary variables $\{u1, u2, u3, u4\}$ defined in Equation's $3.6 - 3.9$**,** can be written as

$$\begin{bmatrix} u_1 \\ u_2 \\ u_3 \\ u_4 \end{bmatrix} = \begin{bmatrix} b & b & b & b \\ 0 & b & 0 & -b \\ b & 0 & -b & 0 \\ d & -d & d & -d \end{bmatrix} \begin{bmatrix} \omega_1^2 \\ \omega_2^2 \\ \omega_3^2 \\ \omega_4^2 \end{bmatrix} \approx \begin{bmatrix} 1 & 1 & 1 & 1 \\ 0 & 1 & 0 & -1 \\ 1 & 0 & -1 & 0 \\ 1 & -1 & 1 & -1 \end{bmatrix} \begin{bmatrix} P_1 \\ P_2 \\ P_3 \\ P_4 \end{bmatrix}$$

Where $P1, P2, P3, P4$ are the motors power. Motors power can then be found from the auxiliary variables as follows

$$\begin{bmatrix} P_1 \\ P_2 \\ P_3 \\ P_4 \end{bmatrix} = \begin{bmatrix} 1 & 0 & 2 & 1 \\ 0 & 2 & 0 & -1 \\ 1 & 0 & -2 & 0 \\ 1 & -2 & 1 & -1 \end{bmatrix} \begin{bmatrix} u_1 \\ u_2 \\ u_3 \\ u_4 \end{bmatrix} = \Gamma \mathrm{U}$$

The matrix Γ maps the auxiliary control actions U, to the proper individual motor control command signal.

The control loops are illustrated in Figure 4.1. The first control loop comprises an RoP controller method (701) which produces a control action (721) corresponding to the auxiliary variable u_1. The produced action is based on the error between the desired RoP_D (709) and the actual RoP (719). The control action is modified based on the Force on Bit (FoB) (741), as measured by the MWD instruments (720). The loop action is

adjusted based on the available FOB, as usually the motors are not enough to achieve the required RoP.

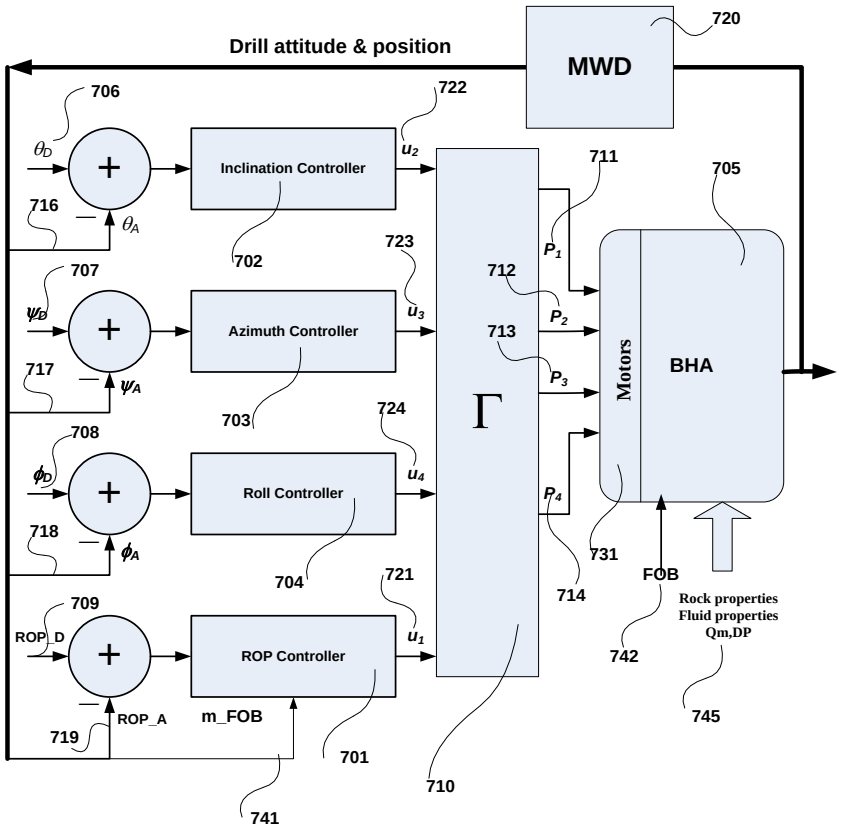

Figure 4.1: Control loops of the quad motors steering system

The second control loop comprises an inclination controller method (702) which produces a control action (722) corresponding to the auxiliary variable u_2. The produced action is based on the error between the desired inclination angle θ_D (706) and the actual inclination θ_A (716). The actual inclination is obtained from the MWD (720).

The third control loop comprises an azimuth angle controller method (703) which produces a control action (723) corresponding to the auxiliary variable u_4. The produced

action is based on the error between the desired azimuth angle ψ_D (707) and the actual inclination ψ_A(717). The actual azimuth is obtained from the MWD (720).

The forth control loop comprises a Roll angle controller method (704) which produces a control action (724) corresponding to the auxiliary variable u_4. The produced action is based on the error between the desired Roll angle ϕ_D(708) and the actual roll angle ϕ_A(718). The actual roll angle is obtained from the MWD (720).

The control actions $\{u_1, u_2, u_3, u_4\}$ are then transformed by the matrix Γ into the motor control commands $P1$ (711), $P2$ (712), $P3$ (713), and $P4$ (714), and transmitted to the motors and motor drivers (731) in the BHA (705). The control loops adjust the control actions in the presence of many operation and environment factors. Environmental Factors include: depth and formation (rock) properties, while operational factors include Bit Wear State, Bit Design, Mud properties, mud flow rate, Bottom hole mud pressure, and weight on bit.

In nonlinear control, the concept of feedback plays a fundamental role in controller design, as it does in linear control. However, the importance of feedforward is much more conspicuous than in linear control. Feedforward is used to cancel the effects of known disturbances and provide anticipative actions in tracking tasks. Very often it is impossible to control a nonlinear system stably without incorporating feedforward action in the control law. Note that a model of the plant is always required for feedforward compensation (although the model need not be very accurate).

Asymptotic tracking control always requires feedforward actions to provide the forces necessary to make the required motion. It is interesting to note that many tracking controllers can be written in the form

u = feedforward + feedback

or in a similar form. The feedforward part intends to provide the necessary input for following the specified motion trajectory and canceling the effects of the known disturbances. The feedback part then stabilizes the tracking error dynamics.

Feedback linearization can be used as a nonlinear design methodology. The basic idea is to first transform a nonlinear system into a (fully or partially) linear system, and then use the well-known and powerful linear design techniques to complete the control design. The approach has been used to solve a number of practical nonlinear control problems. It applies to important classes of nonlinear systems (so-called input-state linearizable or minimum-phase systems), and typically requires full state measurement.

4.2 Feedback Linearization Controller (FLC)

Feedback linearization is an approach to nonlinear control design which has attracted a great deal of research interest in recent years. The central idea of the approach is to algebraically transform a nonlinear system dynamics into a (fully or partly) linear one, so that linear control techniques can be applied. This differs entirely from conventional linearization *(*i.e., Jacobian linearization) in that feedback linearization is achieved by exact state transformations and feedback, rather than by linear approximations of the dynamics. The idea of simplifying the form of a system's dynamics by choosing a different state representation is not entirely unfamiliar. In mechanics, for instance, it is well known that the form and complexity of a system model depend considerably on the choice of reference frames or coordinate systems. Feedback linearization techniques can

be viewed as ways of transforming original system models into equivalent models of a simpler form.

FLC has been used successfully to address some practical control problems. These include the control of helicopters, high performance aircraft, industrial robots, and biomedical devices. More applications of the methodology are being developed in industry. However, there are also a number of important shortcomings and limitations associated with the feedback linearization approach. Such problems are still very much topics of current research.

4.2.1 Input output Linearization

In the MIMO case, we consider, square systems *(i.e.*, systems with the same number of inputs and outputs) of the form

$$\dot{x} = f(k) + G(k)u \tag{4.1}$$

$$y = h(k) \tag{4.2}$$

Where, x is $n \times 1$ the state vector, u is the $m \times 1$ control input vector (of componentsu_i), y is the $m \times 1$ vector of system outputs (of components y_i), f and h are smooth vector fields, and G is a$n \times m$ matrix whose columns are smooth vector fields g_i.

Our objective is to make the output $y(t)$ track a desired trajectory $y_d(t)$ while keeping the whole state bounded. An apparent difficulty with this model is that the output y is only indirectly related to the input u, through the state variable k and the nonlinear state equations $4.1 - 4.2$. Therefore, it is not easy to see how the input's u_i can be designed to

control the tracking behavior of the output y. The difficulty of the tracking control design can be reduced if we can find a direct and simple relation between the system output y and the control input u. Indeed, this idea constitutes the intuitive basis for the so-called input-output linearization approach to nonlinear control design.

By considering the non-linear state equations $3.23 - 3.26$, from the previous chapter, we have a state vector $k = (\ddot{z}, \ddot{\phi}, \ddot{\theta}, \ddot{\psi})$, to achieve the station keeping tracking control for the position outputs (z, ϕ, θ, ψ). We select the output vector $y = (z, \phi, \theta, \psi)$.

To obtain the desired linear equations, one has to differentiate outputs until input vector u appears, i.e. for the set of output $y = h(k)$ with $h \in R^m$ if

$$\ddot{y} = M(k) + E(k).u_i \tag{4.3}$$

Then the desired input which cancel the nonlinearities in the system is obtained as

$$u_i^* = E(k)^{-1}(-M(k) + w_i) \tag{4.4}$$

where $E(k) \in R^{m \times m}$ and $M(k) \in R^{m \times 1}$. $w_i, i = 1,2,3,4$ is the input to the linear controller. Since the input w_i only affects the output y_i, it is called a decoupling control law. The full state feedback linearization is achieved if matrix $E(k)$ is invertible. If relative degree r is equal to the order of the system n, then the matrix $E(k)$ is invertible and the invertible matrix $E(k)$ is called the decoupling matrix of the system. We have relative degree r is equal to the state order of the system n, i.e. 4. So we don't have internal dynamics in the system. Now we can achieve full state feedback linearization control.

Differentiating the output vector twice with respect to the time, we obtain from the equations $3.23 - 3.26$ that

$$\ddot{y} = \begin{bmatrix} \ddot{z} \\ \ddot{\phi} \\ \ddot{\theta} \\ \ddot{\psi} \end{bmatrix} = M_j + E_j u_i^* \tag{4.5}$$

where

$$M_j = \begin{bmatrix} -g\cos\theta - F_{fw}\cos\theta \\ \dot{\theta}\dot{\psi}\frac{I_y - I_z}{I_x} - I_r/I_x\dot{\theta}g(u) \\ \dot{\phi}\dot{\psi}(I_z - I_x/I_y) - I_r/I_y\dot{\psi}g(u) \\ \frac{\dot{\phi}\dot{\theta}(I_x - I_y)}{I_z} - T_{fw,\psi} \end{bmatrix} \tag{4.6}$$

$$E_j = \begin{bmatrix} \frac{1}{m}\cos\theta & 0 & 0 & 0 \\ 0 & L_b/I_x & 0 & 0 \\ 0 & 0 & L_b/I_y & 0 \\ 0 & 0 & 0 & \frac{L_b}{I_z} \end{bmatrix} \tag{4.7}$$

$$u_i^* = \begin{bmatrix} u_1^* \\ u_2^* \\ u_3^* \\ u_4^* \end{bmatrix}$$

We separate attitude control and the RoP control as two levels :

In attitude control level we have the output vector

$$y_1 = \begin{bmatrix} \phi \\ \theta \\ \psi \end{bmatrix}$$

and the input to the Linearized system

$$w_O = \begin{bmatrix} w_\phi \\ w_\theta \\ w\psi \end{bmatrix}.$$

By differentiating the output vector $y_1$twice with respect to time, the equations can be written as

$$\ddot{y_1} = w_o$$

Now we can write the desired input to the system as

$$u_A = E_A^{-1}(-M_A + w_o) \tag{4.8}$$

where

$$E_A = \begin{bmatrix} L_b/I_x & 0 & 0 \\ 0 & L_b/I_y & 0 \\ 0 & 0 & L_b/I_z \end{bmatrix}$$

$$M_A = \begin{bmatrix} \dot{\theta}\dot{\psi}\dfrac{I_y - I_z}{I_x} - I_r/I_x\dot{\theta}g_y \\ \dot{\phi}\dot{\psi}(I_z - I_x/I_y) \; - I_r/I_y\dot{\psi}g_y \\ \dfrac{\dot{\phi}\dot{\theta}\left(I_x - I_y\right)}{I_z} - T_{fw,\psi} \end{bmatrix}$$

The new input variables required to cancel the nonlinearities for the attitude control level are

$$u_A = \begin{bmatrix} u_2^* \\ u_3^* \\ u_4^* \end{bmatrix}$$

where

$$u_2^* = \frac{w_\phi . I_x}{L_b} + \frac{\frac{I_r}{I_x}\dot{\theta} g_y . I_x}{L_b} - \frac{\dot{\theta}\dot{\psi}\left(\frac{I_y - I_z}{I_x}\right).I_x}{L_b} \tag{4.9}$$

$$u_3^* = \frac{w_\theta . I_y}{L_b} - \frac{\dot{\phi}\dot{\psi}\left(\frac{I_z - I_x}{I_y}\right).I_y}{L_b} - \frac{\frac{I_r}{I_y}\dot{\psi} g_y . I_y}{L_b} \tag{4.10}$$

$$u_4^* = \frac{w_\psi . I_z}{L_b} - \frac{\dot{\phi}\dot{\theta}\left(\frac{I_x - I_y}{I_z}\right).I_z}{L_b} + T_{fw,\psi} . \frac{I_z}{L_b} \tag{4.11}$$

For RoP controller level we have output $y_2 = \dot{z}$ and the input to the linearized system is w_z. By differentiating the output with respect to time we obtain the desired input to the system.

Now we can write the desired input to the system as

$$u_1^* = E_Z^{-1}(-M_z + w_o) \tag{4.12}$$

where

$$E_Z = [\frac{1}{m} cos\theta]$$

and

$$M_z = -gcos\theta - F_{fw} cos\theta$$

The new input variable for the Rate of penetration controller is derived as

$$u_1^* = w . m - m . F_{fw} + mgcos\theta \tag{4.13}$$

4.3 Linear Optimal Control

After cancelling the nonlinear dynamics with new input variables using feedback linearization technique now we have to design the linear controller and we have the inputs for the linear system w_A and w_z for attitude control and the rate of penetration control respectively.

First we construct the canonical form for the both attitude control and the Rate of penetration (RoP) control.

The control canonical form for the attitude control can be written as

$$\begin{bmatrix} \dot{\phi} \\ \ddot{\phi} \\ \dot{\theta} \\ \ddot{\theta} \\ \dot{\psi} \\ \ddot{\psi} \end{bmatrix} = \begin{bmatrix} 0 & 1 & 0 & 0 & 0 & 0 \\ 0 & 0 & 0 & 0 & 0 & 0 \\ 0 & 0 & 0 & 1 & 0 & 0 \\ 0 & 0 & 0 & 0 & 0 & 0 \\ 0 & 0 & 0 & 0 & 0 & 1 \\ 0 & 0 & 0 & 0 & 0 & 0 \end{bmatrix} \begin{bmatrix} \phi \\ \dot{\phi} \\ \theta \\ \dot{\theta} \\ \psi \\ \dot{\psi} \end{bmatrix} + \begin{bmatrix} 0 & 0 & 0 \\ 1 & 0 & 0 \\ 0 & 0 & 0 \\ 0 & 1 & 0 \\ 0 & 0 & 0 \\ 0 & 0 & 1 \end{bmatrix} \begin{bmatrix} w_\phi \\ w_\theta \\ w_\psi \end{bmatrix}$$

The control canonical form for the RoP control can be written as

$$\begin{bmatrix} \dot{z} \\ \ddot{z} \end{bmatrix} = \begin{bmatrix} 0 & 0 \\ 0 & 1 \end{bmatrix} \begin{bmatrix} z \\ \dot{z} \end{bmatrix} + \begin{bmatrix} 0 \\ 1 \end{bmatrix} w_z$$

The state space form of the above canonical forms is given as

$$\dot{X}_A = AX_A + Bw_O \quad \text{and}$$

$$\dot{X}_z = AX_z + Bw_z$$

for both attitude and RoP controllers.

And in state feedback inputs for the attitude and RoP controllers are given as

$$w_A = -K_A.X_A \quad \text{and}$$

$$w_z = -K_z.X_z$$

where

$K_A \; and \; K_z$ are the constant gains.

4.3.1 Linear Quadratic Regulator (LQR)

The LQR is used to calculate the gains K_A and K_z .For the derivation of the linear quadratic regulator, we assume the model to be written in state-space form $\dot{X}_A = AX_A + Bw_O$ and $\dot{X}_z = AX_z + Bw_z$ for both attitude and RoP controllers.and that all of the n states are available for the controller. The feedback gain is a matrix $K_A \; and \; K_z$ implemented as

$$w_A = -K_A.(X_A - X_{dA}) \quad \text{and}$$

$$w_z = -K_z.(X_z - X_{dz})$$

Where X_{dA} and X_{dz} are the reference signals for tracking, and serves as the external input to the closed loop system.

$$X_{dA} = [\psi_D, \theta_D, \phi_D]$$

$$X_{dz} = RoP_D$$

The system dynamics are then written as:

$$\dot{X}_A = (A - BK_A)X_A + BK_A.X_{DA} \tag{4.14}$$

for the attitude controller and

$$\dot{X}_z = (A - BK_z)X_z + BK_z.X_{Dz} \tag{4.15}$$

for RoP controller. The block diagram of LQR controller in shown in Figure 4.2.

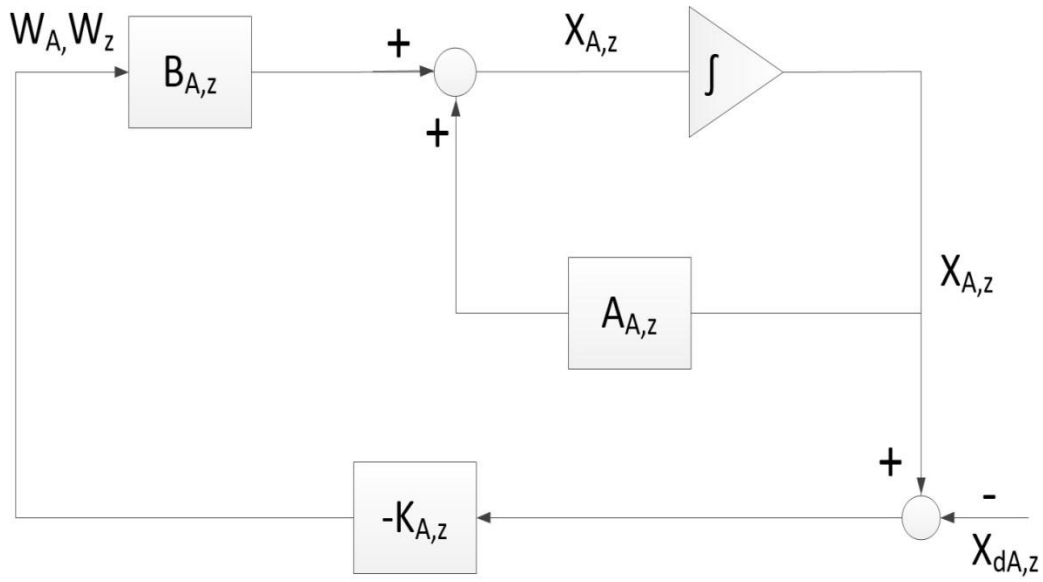

Figure 4.2: structure of LQR controller

Let us consider the closed loop system $\dot{X}_A = AX_A + Bw_O$ for attitude controller. Lyapunav function guaranteed the stability of the closed system.

$$V(X_A) = X_A^T P X_A$$

$$\dot{V} = \dot{X}_A^T P X_A + X_A^T P \dot{X}$$

$$= [(A - BK_A)X_A^T]^T P X_A + X_A^T P[(A - BK_A)X_A]$$

$$= X_A^T[(A - BR^{-1}B^T P)^T P + P(A - BR^{-1}B^T P)]X_A$$

$$= X^T[(PA + A^T P - PBR^{-1}B^T P + Q) - Q - PBR^{-1}B^T P]X_A$$

$$= X_A^T[-Q - PBR^{-1}B^T P]X_A$$

for $R > 0, \quad R^{-1} > 0$. Also $P > 0$

So, $PBR^{-1}B^{T}P > 0$

Also $\quad Q \geq 0.$

Hence, $PBR^{-1}B^{T}P + Q > 0$

where

P is the positive symmetric matrix.

$Q\ and\ R$ are positive definite matrix's compatible with the dimensions of A and B matrices of the closed loop system.

Therefore $\dot{V}(X_A) < 0$. Hence the closed loop system is always asymptotically stable.

The minimum value of cost function is given as

$$J_A = \frac{1}{2}\int_{t_0}^{\infty} (X_A^T Q X_A + w_o^T R w_o) dt$$

$$= \frac{1}{2}\int_{t_0}^{\infty} [\, X_A^T Q X_A + (-R^{-1}B^T P X_A)^T \, R(-R^{-1}B^T P X_A)] dt$$

$$= \frac{1}{2}\int_{t_0}^{\infty} X_A^T (Q + PBR^{-1}B^T P) X_A dt$$

$$J_A = \frac{1}{2}\int_{t_0}^{\infty} \left(-\dot{V}_A\right) dt$$

$$= \tfrac{1}{2}\left[X_{A_0}^T P X_{A_0} - X_{A_\infty}^T P X_{A_\infty}\right] = \tfrac{1}{2}(X_{A_0}^T P X_{A_0}).$$

Similarly for the RoP controller closed loop system, we can guaranteed the stability by using Lyapunav function.

The objective cost function for tracking some desired trajectory can be formulated as

$$J_A = \frac{1}{2}\int_{t_0}^{\infty}((X_A^T - X_{dA})Q(X_A - X_{dA}) + w_o^T R w_o)dt \qquad (4.16)$$

and

$$J_Z = \frac{1}{2}\int_{t_0}^{\infty}((X_Z^T - X_{dz})Q(X_z - X_{dz}) + w_z^T R w_z)dt \qquad (4.17)$$

for both attitude and RoP controllers.

The overall control system in shown in Figure 4.3

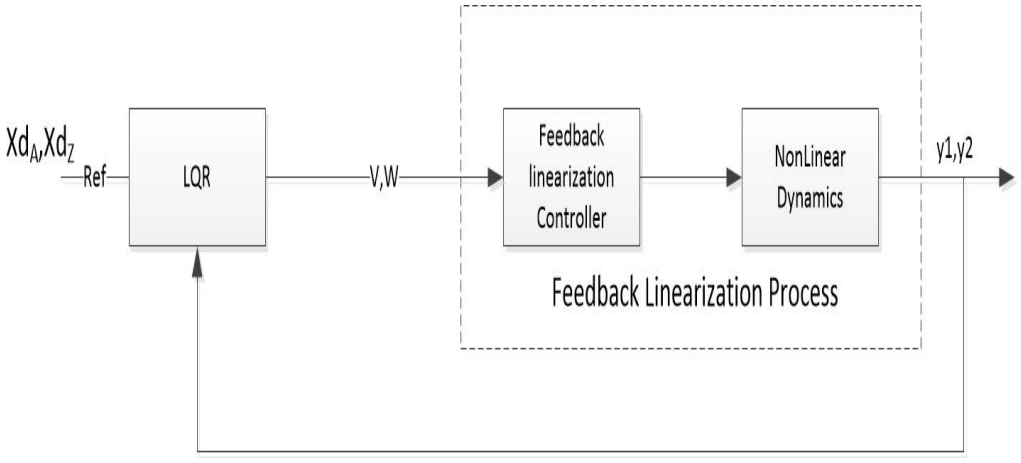

Figure 4.3: Overall control system for DSS

4.4 Tracking a trajectory

To verify the proposed controller, simulations were shown using the reference signal as the desired trajectory for measured distance, inclination and azimuth. The data for reference trajectory is given in Appendix IV. The actual responses with their references

were shown in Figure 4.8, 4.9 and 4.10. The DSS model using the parameters of Table 3.1 is then implemented in Matlab/Simulink. The first set of simulations in Figure's $(4.4 - 4.7)$ show the histories of the control inputs.

.

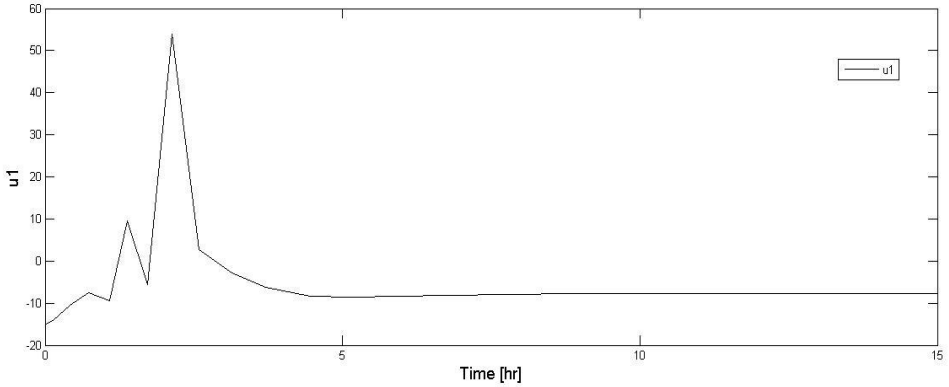

Figure 4.4: Control input u_1

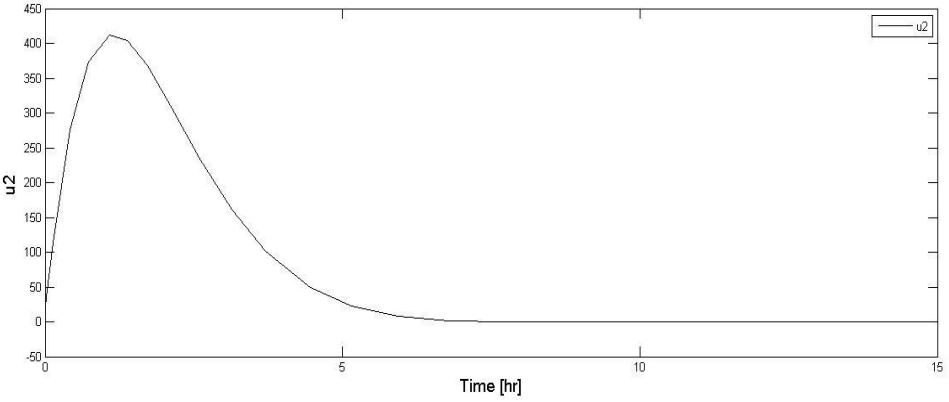

Figure 4.5: Control input u_2

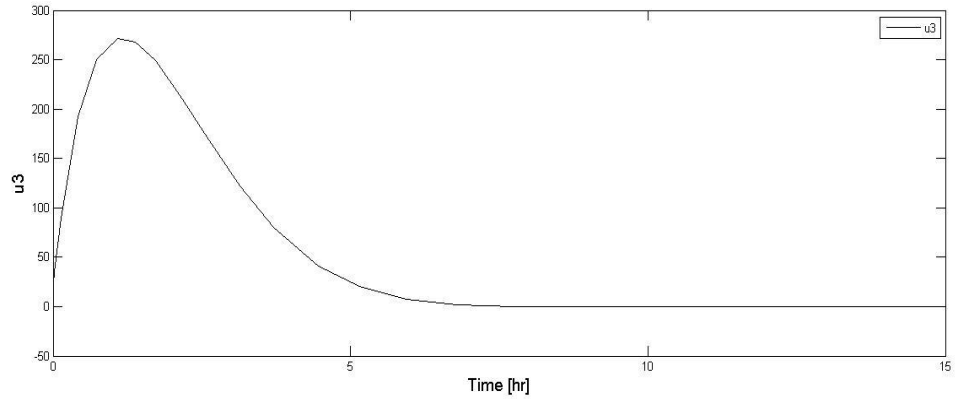

Figure 4.6: Control input u_3

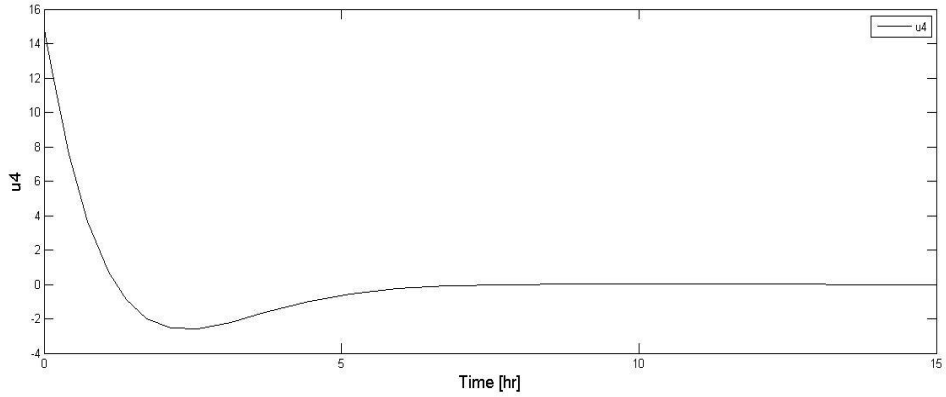

Figure 4.7: Control input u_4.

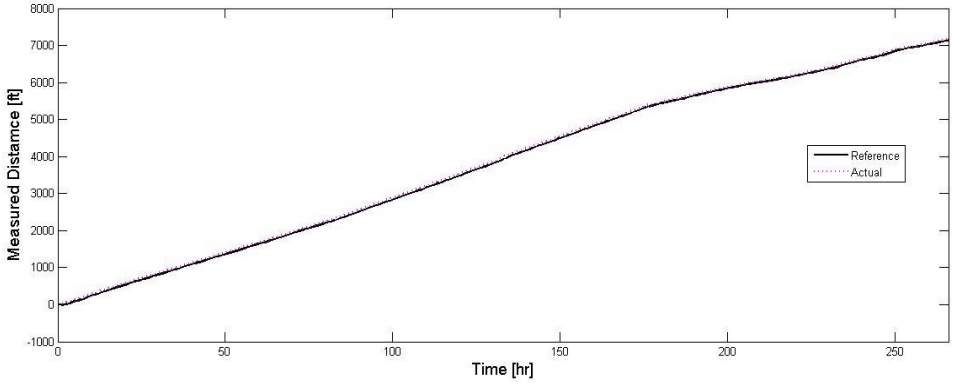

Figure 4.8: Time plot of measured distance actual and measured distance reference

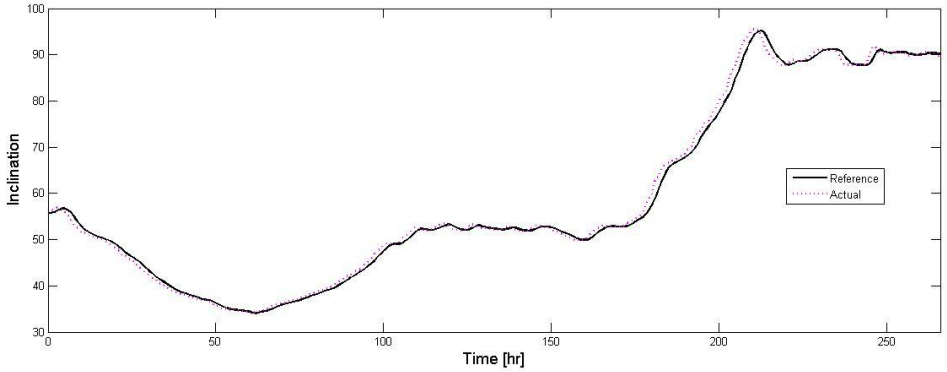

Figure 4.9: Time plot of Inclination actual and Inclination reference

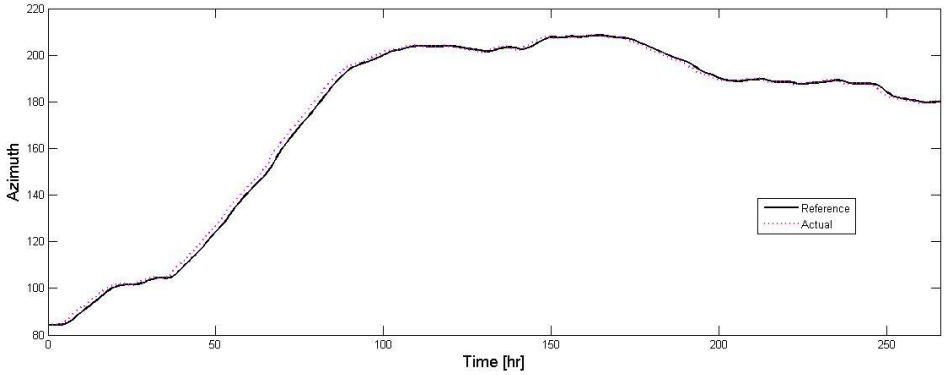

Figure 4.10: Time plot of azimuth actual and azimuth reference

With the help of SES software [75], by entering data of desired measured distance, inclination and azimuth, we obtained the directional well planning and values of True vertical Depth (TVD), east and north. Using the data obtained from SES software we generate a 3D simulation of $\dot{w}$ (RoP) as shown in Figure 4.12. Data obtained from SES software was presented in Appendix IV.

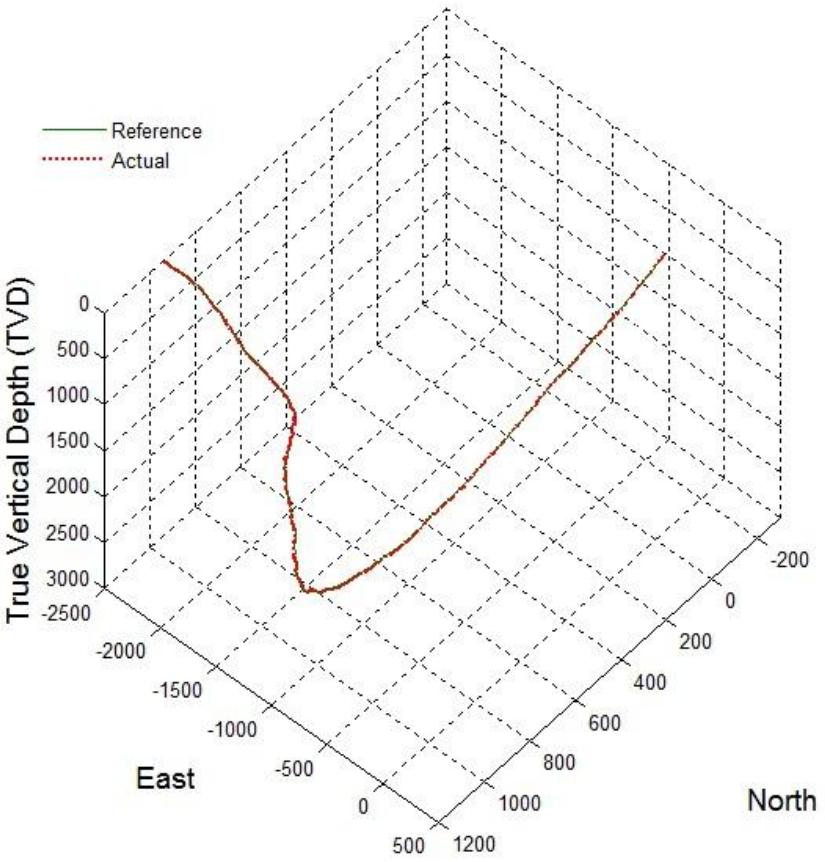

Figure 4.11: 3D view of the RoP tracking

CHAPTER 5

CONCLUSIONS

A model for the DSS is developed where in drilling head comprises four motors driving four drill bits, and where in the rotational speed of the each motor is independently controlled causing the rate of removal of rocks and the direction of the advancement of the drilling head to be precisely controlled, wherein two motors rotate CW, and the other two motors rotate CCW for control of the roll angle of the drilling head, and where in the drill head assembly is connected to drill string, which includes the inner pipe for carrying the drilling fluid, and comprising a drill head control method which translates the steering commands in the form of desired inclination angle, desired azimuth angle, roll position, and rate of penetration to individual motor commands and the model is not yet completely established in the literature. A controller to control the DSS was designed by Feedback Linearization controller to cancel the non-linear dynamics and the LQR was selected for the optimal linear control. FLC-LQR controller works very well and tracks the desired trajectory and RoP control for DSS.

5.1 Future Work

The interaction-interface between the rocks and the rest of the drilling system is both extensive and complex, it undergoes change as it does work, as it is mixed with fluids from the rock, as it undergoes pressure and temperature changes and as it cycles between down hole and the surface where chemicals are added and removed. These changes can be considered in the Modeling of DSS. The effect of disturbance can be modeled and the controller can be tested against disturbances. Optimization of RoP can be obtained by using an optimization technique. Also, the control techniques for DSS can be considered.

APPENDICES

I. Simulink Model for DSS control

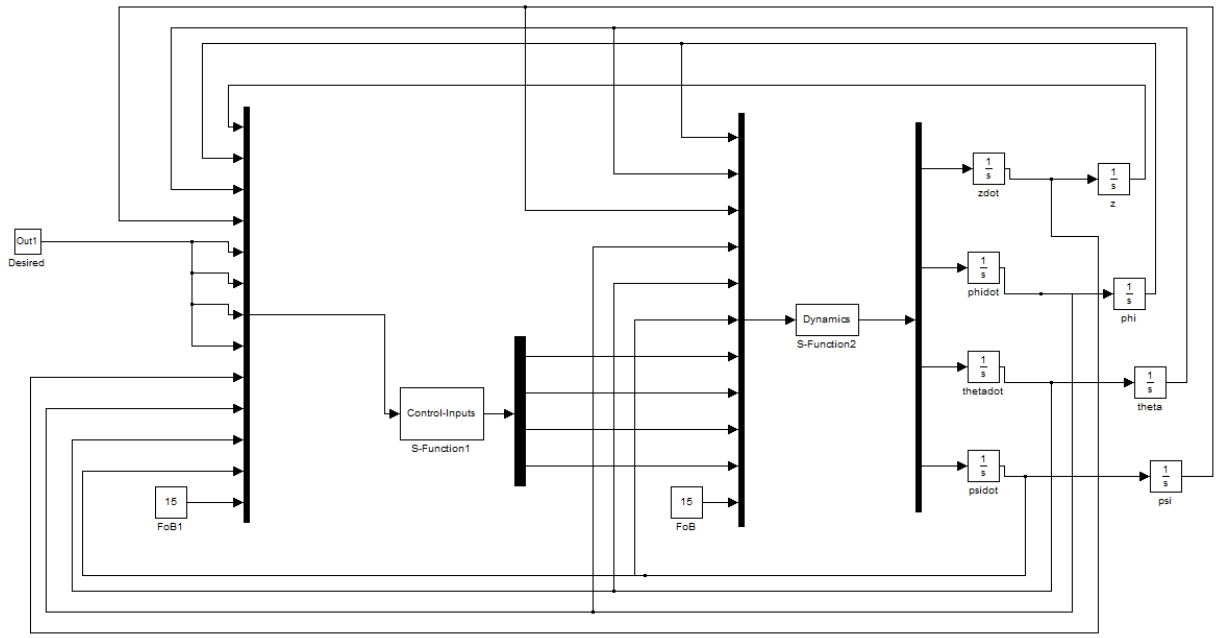

II. Dynamics S-function Matlab code

```
function [sys,x0,str,ts,simStateCompliance] = Dynamics(t,x,u,flag)
 switch flag,
  % Initialization %
  case 0,
    [sys,x0,str,ts,simStateCompliance]=mdlInitializeSizes;
```

```
 % Outputs %
 case 3,
   sys=mdlOutputs(t,x,u);
 case { 1, 2, 4, 9 }
   sys=[];
 % Unexpected flags %
 otherwise
   DAStudio.error('Simulink:blocks:unhandledFlag', num2str(flag));
end
% end sfuntmpl
% mdlInitializeSizes
% Return the sizes, initial conditions, and sample times for the S-function.
function [sys,x0,str,ts,simStateCompliance]=mdlInitializeSizes
 sizes = simsizes;
sizes.NumContStates  = 0;
sizes.NumDiscStates  = 0;
sizes.NumOutputs     = 4;
sizes.NumInputs      = 11;
sizes.DirFeedthrough = 1;
sizes.NumSampleTimes = 1;   % at least one sample time is needed
sys = simsizes(sizes);

x0  = [];
```

```
str = [];

ts  = [0 0];

% Specify the block simStateCompliance. The allowed values are:
%    'UnknownSimState', < The default setting; warn and assume      DefaultSimState
%    'DefaultSimState', < Same sim state as a built-in block
%    'HasNoSimState',   < No sim state
%    'DisallowSimState' < Error out when saving or restoring the model sim state
simStateCompliance = 'UnknownSimState';
 function sys=mdlOutputs(t,x,u)

      %%%%% Parameters %%%%%

m=200;
ix=60;
iy=60;
iz=25;
g=9.80;
ir=0.83;
l=0.2;
mu=0.25;
```

```
gu=50;

        %%%%% States and Inputs %%%%%

 phi = u(1);

theta = u(2);

psi = u(3);

phidot=u(4);

thetadot=u(5);

psidot=u(6);

u1= u(7);

u2=u(8);

u3=u(9);

u4=u(10);

FoB=u(11);

        %%%%% State Space Model %%%%%

 Ffw=(sin(theta)*cos(psi)*m*g + sin(theta)*sin(phi)*m*g)*mu;

 rt=(-cos(psi)*sin(theta)*cos(phi)+sin(psi)*sin(phi));

zddot=(u1*rt/m)+FOB*rt-Ffw+m*g*cos(theta);

phiddot=(((iy-iz)/ix)*psidot*thetadot)-ir*gu*thetadot +l*u2;

thetaddot=(((iz-ix)/iy)*psidot*phidot)-ir*gu*phidot +l*u3;


psiddot=(((ix-iy)/iz)*phidot*thetadot)+l*u4;
```

```
xdot = [zddot;phiddot;thetaddot;psiddot];

sys = xdot;
```

III. Control-Inputs S-function Matlab code

```
function [sys,x0,str,ts,simStateCompliance] = Control-Inputs(t,x,u,flag)

 switch flag,


    % Initialization %

  case 0,

    [sys,x0,str,ts,simStateCompliance]=mdlInitializeSizes;


  % Outputs %

  case 3,

    sys=mdlOutputs(t,x,u);


  case { 1, 2, 4, 9 }

    sys=[];


  % Unexpected flags %

  otherwise

    DAStudio.error('Simulink:blocks:unhandledFlag', num2str(flag));

end
```

```
% end sfuntmpl

 % mdlInitializeSizes

% Return the sizes, initial conditions, and sample times for the S-function.


function [sys,x0,str,ts,simStateCompliance]=mdlInitializeSizes

sizes = simsizes;

sizes.NumContStates  = 0;

sizes.NumDiscStates  = 0;

sizes.NumOutputs     =4;

sizes.NumInputs      = 13;

sizes.DirFeedthrough = 1;

sizes.NumSampleTimes = 1;   % at least one sample time is needed

sys = simsizes(sizes);

 x0  = [];

 str = [];

ts  = [0 0];


% Specify the block simStateCompliance. The allowed values are:

%    'UnknownSimState', < The default setting; warn and assume DefaultSimState

%    'DefaultSimState', < Same sim state as a built-in block

%    'HasNoSimState',   < No sim state

%    'DisallowSimState' < Error out when saving or restoring the model sim state
```

```
simStateCompliance = 'UnknownSimState';


 function sys=mdlOutputs(t,x,u)


      %%%%% Parameters %%%%%
 m=200;
ix=60;
iy=60;
iz=25;
g=9.80;
ir=0.83;
l=0.2;
mu=0.25;
gu=50;


      %%%%% States and Inputs %%%%%
z1 = u(1);
phi=u(2);
theta=u(3);
psi= u(4);
z1r = u(5);
phir=u(6);
psir=u(7);
```

```
thetar=u(8);

z1dot=u(9);

phidot=u(10);

thetadot=u(11);

psidot=u(12);

FOB=u(13);


      %%%%% State Space Model %%%%%


A1=[0 1;0 0];

B1=[0; 1];

Q1=300*eye(2);

R1=600*eye(1);

[K1,S1,e1] = lqr(A1,B1,Q1,R1);

X1=[z1;z1dot];

w=z1r-K1*X1;

 Ffw=(sin(theta)*cos(psi)*m*g+sin(theta)*sin(phi)*m*g)*mu;

 rt=(-cos(psi)*sin(theta)*cos(phi)+sin(psi)*sin(phi));

 u1=(w*m)/rt-((FOB*m)/rt)+(Ffw*m)-(m*g*cos(theta)/rt);

A=[0 1 0 0 0 0;0 0 0 0 0 0 ;0 0 0 1 0 0;0 0 0 0 0 0;0 0 0 0 0 1;0 0 0 0 0 0];

B=[0 0 0;1 0 0;0 0 0;0 1 0;0 0 0;0 0 1];

Q=eye(6);

R=eye(3);
```

```
[K,S,e] = lqr(A,B,Q,R);

X=[phi;phidot;theta;thetadot;psi;psidot];

r=[phir;thetar;psir];

v=r-K*X;

 v1=v(1);

v2=v(2);

v3=v(3);

u2=v1/l+(ir*gu*thetadot)/l-(((iy-iz)/ix)*psidot*thetadot)/l;

u3=v2/l+(ir*gu*phidot)/l-(((iz-ix)/iy)*psidot*phidot)/l;

u4=v3/l-(((ix-iy)/iz)*phidot*thetadot)/l;

sys =[u1;u2;u3;u4];
```

IV. Data obtained from SES software

Measured Distance (MD)*	Inclination INC*	Azimuth AZI*	True Vertical Depth TVD*	North (N)*	East (E)*
0.00	56.19	84.34	0.00	0.00	0.00
50.00	56.67	84.38	27.65	4.09	41.46
90.88	57.06	84.42	49.99	7.43	75.53
100.00	56.78	84.74	54.97	8.15	83.13
131.23	55.81	85.87	72.30	10.28	109.03
150.00	55.24	86.56	82.93	11.30	124.47
200.00	53.73	88.45	111.98	13.08	165.12
234.58	52.70	89.80	132.69	13.50	192.81

250.00	52.39	90.38	142.06	13.48	205.05
300.00	51.40	92.29	172.92	12.57	244.38
300.20	51.40	92.30	173.04	12.57	244.54
350.00	50.97	93.98	204.26	10.44	283.28
394.36	50.60	95.50	232.31	7.60	317.53
400.00	50.55	95.75	235.89	7.17	321.86
450.00	50.16	97.96	267.80	2.58	360.08
457.68	50.10	98.30	272.72	1.75	365.92
500.00	49.47	99.95	300.04	-3.37	397.82
519.03	49.20	100.70	312.44	-5.96	412.03
550.00	48.66	101.04	332.79	-10.36	434.95
581.69	48.10	101.40	353.84	-14.97	458.19
600.00	47.63	101.52	366.12	-17.67	471.50
644.03	46.50	101.80	396.11	-24.18	503.07
650.00	46.42	101.76	400.23	-25.07	507.31
700.00	45.78	101.44	434.90	-32.31	542.60
706.04	45.70	101.40	439.11	-33.17	546.84
750.00	44.67	102.15	470.09	-39.53	577.37
770.34	44.20	102.50	484.62	-42.57	591.28
800.00	43.48	103.16	506.01	-47.13	611.31
832.68	42.70	103.90	529.88	-52.35	633.02

850.00	42.36	104.18	542.64	-55.19	644.37
893.37	41.50	104.90	574.91	-62.46	672.43
900.00	41.38	104.83	579.88	-63.59	676.67
950.00	40.52	104.28	617.64	-71.82	708.38
956.69	40.40	104.20	622.73	-72.89	712.59
1000.00	39.64	104.68	655.90	-79.84	739.56
1019.36	39.30	104.90	670.84	-82.98	751.46
1050.00	38.93	106.87	694.62	-88.27	770.05
1079.72	38.60	108.80	717.79	-93.96	787.76
1100.00	38.43	109.68	733.66	-98.12	799.69
1143.70	38.10	111.60	767.97	-107.66	825.01
1150.00	38.03	111.95	772.93	-109.10	828.62
1200.00	37.55	114.79	812.45	-121.25	856.74
1205.38	37.50	115.10	816.71	-122.63	859.71
1250.00	37.07	117.35	852.22	-134.57	883.96
1268.70	36.90	118.30	867.15	-139.82	893.91
1300.00	36.88	120.50	892.19	-149.05	910.27
1328.41	36.90	122.50	914.91	-157.96	924.81
1350.00	36.54	123.60	932.22	-164.99	935.63
1390.42	35.90	125.70	964.83	-178.57	955.28
1400.00	35.76	126.26	972.59	-181.86	959.82

1449.48	35.10	129.20	1012.91	-199.41	982.50
1450.00	35.10	129.24	1013.34	-199.60	982.74
1500.00	34.84	133.44	1054.32	-218.51	1004.24
1512.47	34.80	134.50	1064.55	-223.46	1009.37
1550.00	34.73	136.64	1095.39	-238.74	1024.34
1573.82	34.70	138.00	1114.97	-248.71	1033.54
1600.00	34.60	139.53	1136.50	-259.90	1043.35
1633.53	34.50	141.50	1164.12	-274.58	1055.44
1650.00	34.32	142.40	1177.71	-281.90	1061.18
1691.60	33.90	144.70	1212.15	-300.67	1075.04
1700.00	33.98	145.14	1219.12	-304.50	1077.73
1750.00	34.48	147.70	1260.46	-327.93	1093.28
1751.97	34.50	147.80	1262.09	-328.87	1093.88
1800.00	34.71	150.75	1301.62	-352.32	1107.81
1815.62	34.80	151.70	1314.46	-360.12	1112.10
1850.00	35.19	154.61	1342.62	-377.71	1121.00
1900.00	35.88	158.74	1383.32	-404.39	1132.49
1908.14	36.00	159.40	1389.91	-408.85	1134.19
1950.00	36.12	161.97	1423.75	-432.10	1142.34
1971.79	36.20	163.30	1441.34	-444.37	1146.18
2000.00	36.37	165.26	1464.08	-460.44	1150.70

2032.48	36.60	167.50	1490.20	-479.20	1155.24
2050.00	36.74	168.56	1504.25	-489.44	1157.41
2090.88	37.10	171.00	1536.94	-513.60	1161.77
2100.00	37.19	171.55	1544.21	-519.04	1162.60
2150.00	37.73	174.54	1583.90	-549.22	1166.28
2156.17	37.80	174.90	1588.78	-552.98	1166.63
2200.00	38.21	177.90	1623.32	-579.91	1168.32
2217.85	38.40	179.10	1637.32	-590.97	1168.61
2250.00	38.70	181.15	1662.47	-611.01	1168.57
2279.53	39.00	183.00	1685.47	-629.51	1167.90
2300.00	39.12	184.22	1701.36	-642.39	1167.08
2350.00	39.45	187.17	1740.07	-673.88	1163.94
2369.42	39.60	188.30	1755.05	-686.13	1162.28
2400.00	40.01	189.57	1778.54	-705.46	1159.24
2450.00	40.72	191.61	1816.64	-737.29	1153.28
2462.27	40.90	192.10	1825.92	-745.14	1151.63
2500.00	41.43	193.45	1854.33	-769.36	1146.14
2550.00	42.15	195.19	1891.61	-801.64	1137.90
2553.15	42.20	195.30	1893.94	-803.68	1137.34
2600.00	42.85	196.01	1928.47	-834.17	1128.79
2646.33	43.50	196.70	1962.25	-864.59	1119.86

2650.00	43.56	196.76	1964.92	-867.01	1119.14
2700.00	44.43	197.52	2000.88	-900.20	1108.90
2738.52	45.10	198.10	2028.23	-926.02	1100.60
2750.00	45.39	198.34	2036.32	-933.77	1098.05
2800.00	46.66	199.34	2071.03	-967.82	1086.43
2828.74	47.40	199.90	2090.62	-987.63	1079.37
2850.00	47.82	200.38	2104.95	-1002.37	1073.96
2900.00	48.82	201.49	2138.20	-1037.25	1060.61
2923.56	49.30	202.00	2153.64	-1053.78	1054.02
2950.00	49.18	202.09	2170.90	-1072.34	1046.50
3000.00	48.97	202.25	2203.65	-1107.33	1032.25
3015.09	48.90	202.30	2213.57	-1117.86	1027.94
3050.00	49.63	202.85	2236.35	-1142.28	1017.78
3100.00	50.69	203.62	2268.38	-1177.56	1002.63
3105.32	50.80	203.70	2271.74	-1181.33	1000.98
3150.00	51.64	203.89	2299.73	-1213.20	986.93
3200.00	52.58	204.10	2330.44	-1249.25	970.88
3201.12	52.60	204.10	2331.12	-1250.06	970.52
3250.00	52.22	203.89	2360.93	-1285.45	954.77
3292.00	51.90	203.70	2386.75	-1315.76	941.41
3300.00	51.95	203.70	2391.69	-1321.52	938.87
3350.00	52.28	203.70	2422.39	-1357.66	923.01
3382.87	52.50	203.70	2442.45	-1381.50	912.55

3400.00	52.70	203.77	2452.85	-1393.96	907.07
3450.00	53.28	203.98	2482.95	-1430.47	890.91
3477.69	53.60	204.10	2499.45	-1450.78	881.84
3500.00	53.26	203.93	2512.74	-1467.15	874.55
3550.00	52.49	203.55	2542.92	-1503.64	858.50
3569.23	52.20	203.40	2554.66	-1517.60	852.44
3600.00	52.10	203.17	2573.54	-1539.92	842.83
3650.00	51.94	202.79	2604.31	-1576.20	827.45
3661.42	51.90	202.70	2611.36	-1584.49	823.97
3700.00	52.49	202.53	2635.01	-1612.63	812.25
3750.00	53.26	202.31	2665.18	-1649.49	797.05
3752.30	53.30	202.30	2666.56	-1651.19	796.35
3800.00	52.89	201.80	2695.20	-1686.55	782.03
3846.46	52.50	201.30	2723.35	-1720.92	768.46
3850.00	52.49	201.34	2725.51	-1723.54	767.43
3900.00	52.39	201.86	2755.99	-1760.39	752.85
3950.00	52.29	202.38	2786.54	-1797.06	737.94
4000.00	52.19	202.91	2817.16	-1833.54	722.72
4046.59	52.10	203.40	2845.75	-1867.36	708.26
4050.00	52.13	203.40	2847.84	-1869.83	707.19
4100.00	52.53	203.40	2878.40	-1906.15	691.47
4133.20	52.80	203.40	2898.53	-1930.38	680.98
4150.00	52.63	203.15	2908.71	-1942.66	675.70

4200.00	52.14	202.38	2939.22	-1979.18	660.38
4224.74	51.90	202.00	2954.45	-1997.24	653.01
4250.00	51.90	202.58	2970.04	-2015.63	645.47
4300.00	51.90	203.71	3000.89	-2051.81	630.01
4316.93	51.90	204.10	3011.34	-2063.99	624.61
4350.00	52.29	204.98	3031.65	-2087.72	613.77
4400.00	52.90	206.28	3062.03	-2123.53	596.59
4408.46	53.00	206.50	3067.12	-2129.58	593.59
4450.00	52.83	207.14	3092.17	-2159.15	578.64
4500.00	52.62	207.92	3122.46	-2194.43	560.25
4505.25	52.60	208.00	3125.65	-2198.12	558.30
4550.00	52.19	207.65	3152.95	-2229.47	541.75
4593.50	51.80	207.30	3179.73	-2259.88	525.93
4600.00	51.74	207.37	3183.76	-2264.42	523.59
4650.00	51.27	207.88	3214.88	-2299.09	505.44
4689.63	50.90	208.30	3239.77	-2326.29	490.93
4700.00	50.77	208.22	3246.32	-2333.37	487.12
4750.00	50.14	207.82	3278.16	-2367.41	469.01
4777.23	49.80	207.60	3295.67	-2385.87	459.31
4800.00	49.85	207.77	3310.36	-2401.27	451.23
4850.00	49.95	208.13	3342.57	-2435.06	433.30
4873.36	50.00	208.30	3357.59	-2450.82	424.85
4900.00	50.56	208.42	3374.61	-2468.85	415.11

4950.00	51.62	208.64	3406.02	-2503.04	396.53
4963.25	51.90	208.70	3414.22	-2512.17	391.53
5000.00	52.35	208.41	3436.78	-2537.65	377.67
5050.00	52.95	208.03	3467.12	-2572.67	358.87
5053.81	53.00	208.00	3469.41	-2575.35	357.44
5100.00	52.85	207.70	3497.26	-2607.94	340.23
5115.81	52.80	207.60	3506.81	-2619.10	334.38
5150.00	52.80	207.52	3527.48	-2643.24	321.78
5200.00	52.80	207.40	3557.71	-2678.58	303.42
5240.16	52.80	207.30	3581.99	-2706.99	288.72
5250.00	52.95	207.14	3587.93	-2713.97	285.13
5300.00	53.69	206.34	3617.80	-2749.78	267.09
5333.99	54.20	205.80	3637.80	-2774.46	255.02
5350.00	54.45	205.45	3647.14	-2786.19	249.40
5397.97	55.20	204.40	3674.78	-2821.75	232.87
5400.00	55.30	204.34	3675.93	-2823.27	232.19
5429.79	56.80	203.40	3692.57	-2845.87	222.19
5450.00	58.76	202.47	3703.34	-2861.61	215.53
5460.63	59.80	202.00	3708.77	-2870.07	212.07
5491.47	63.00	201.30	3723.54	-2895.23	202.08
5500.00	63.70	201.00	3727.36	-2902.34	199.33
5522.97	65.60	200.20	3737.19	-2921.78	192.03

5550.00	66.37	199.34	3748.19	-2945.01	183.68
5554.46	66.50	199.20	3749.98	-2948.87	182.33
5584.97	67.00	198.10	3762.02	-2975.43	173.37
5600.00	67.22	197.93	3767.87	-2988.60	169.09
5647.64	67.90	197.40	3786.06	-3030.55	155.72
5650.00	67.96	197.30	3786.94	-3032.64	155.07
5679.79	68.70	196.00	3797.94	-3059.16	147.14
5700.00	69.69	195.07	3805.12	-3077.36	142.08
5710.30	70.20	194.60	3808.65	-3086.72	139.60
5742.78	72.90	192.80	3818.93	-3116.65	132.31
5750.00	73.20	192.64	3821.04	-3123.38	130.79
5774.28	74.20	192.10	3827.85	-3146.15	125.80
5800.00	75.43	191.53	3834.59	-3170.44	120.72
5805.77	75.70	191.40	3836.03	-3175.92	119.61
5835.96	77.20	190.40	3843.10	-3204.74	114.06
5850.00	78.46	189.90	3846.06	-3218.25	111.64
5867.13	80.00	189.30	3849.26	-3234.84	108.83
5896.00	81.20	189.00	3853.98	-3262.96	104.31
5900.00	81.62	189.00	3854.57	-3266.87	103.69
5927.17	84.50	189.00	3857.86	-3293.50	99.47

5950.00	86.82	188.71	3859.58	-3315.99	95.96
5958.66	87.70	188.60	3860.00	-3324.54	94.66
5977.69	90.09	189.07	3860.37	-3343.34	91.74
6000.00	92.89	189.62	3859.79	-3365.35	88.12
6003.28	93.30	189.70	3859.61	-3368.58	87.57
6020.34	94.50	189.48	3858.45	-3385.36	84.73
6034.45	95.50	189.30	3857.22	-3399.23	82.44
6050.00	95.41	189.91	3855.74	-3414.49	79.86
6052.17	95.40	190.00	3855.54	-3416.62	79.48
6080.05	93.20	189.30	3853.44	-3444.02	74.82
6100.00	91.25	188.69	3852.67	-3463.71	71.71
6112.86	90.00	188.30	3852.53	-3476.43	69.81
6122.70	89.40	188.30	3852.58	-3486.17	68.39
6150.00	88.46	188.56	3853.09	-3513.17	64.39
6154.53	88.30	188.60	3853.22	-3517.64	63.71
6185.37	87.30	188.60	3854.40	-3548.12	59.10
6200.00	87.73	188.46	3855.04	-3562.57	56.94
6216.21	88.20	188.30	3855.61	-3578.60	54.57
6247.70	89.00	187.20	3856.38	-3609.79	50.33
6250.00	88.95	187.25	3856.42	-3612.07	50.04

6278.54	88.30	187.90	3857.11	-3640.35	46.28
6300.00	88.75	187.90	3857.66	-3661.60	43.33
6307.09	88.90	187.90	3857.81	-3668.62	42.36
6339.57	89.80	188.30	3858.18	-3700.78	37.78
6350.00	90.16	188.30	3858.18	-3711.10	36.27
6371.72	90.90	188.30	3857.98	-3732.59	33.14
6400.00	91.18	188.58	3857.47	-3760.56	28.99
6402.23	91.20	188.60	3857.42	-3762.76	28.66
6450.00	91.20	189.17	3856.42	-3809.95	21.28
6460.96	91.20	189.30	3856.19	-3820.76	19.52
6500.00	91.07	189.30	3855.42	-3859.28	13.21
6520.67	91.00	189.30	3855.04	-3879.68	9.87
6550.00	89.53	188.63	3854.91	-3908.65	5.30
6582.35	87.90	187.90	3855.64	-3940.65	0.65
6600.00	87.85	187.74	3856.29	-3958.13	-1.75
6614.83	87.80	187.60	3856.85	-3972.81	-3.72
6646.65	87.80	187.90	3858.08	-4004.32	-8.01
6650.00	87.79	187.90	3858.20	-4007.64	-8.47
6677.17	87.70	187.90	3859.27	-4034.53	-12.20
6700.00	87.77	187.90	3860.18	-4057.12	-15.34
6709.65	87.80	187.90	3860.55	-4066.67	-16.66
6750.00	90.59	187.43	3861.12	-4106.66	-22.05
6770.34	92.00	187.20	3860.66	-4126.82	-24.64
6800.00	91.38	186.07	3859.78	-4156.27	-28.06
6850.00	90.35	184.15	3859.02	-4206.06	-32.51

6861.88	90.10	183.70	3858.98	-4217.92	-33.33
6894.36	90.40	181.90	3858.84	-4250.36	-34.91
6900.00	90.44	181.90	3858.79	-4255.99	-35.10
6924.87	90.60	181.90	3858.57	-4280.85	-35.93
6945.54	90.53	181.38	3858.37	-4301.51	-36.52
6950.00	90.51	181.27	3858.33	-4305.97	-36.62
6952.76	90.50	181.20	3858.30	-4308.73	-36.68
6988.85	89.80	180.20	3858.21	-4344.81	-37.12
7000.00	89.84	180.32	3858.24	-4355.96	-37.17
7017.72	89.90	180.50	3858.28	-4373.68	-37.30
7046.92	90.00	179.50	3858.31	-4402.88	-37.30
7050.00	90.07	179.53	3858.31	-4405.96	-37.27
7078.08	90.70	179.80	3858.12	-4434.04	-37.11
7100.00	90.42	179.80	3857.90	-4455.96	-37.03
7108.92	90.30	179.80	3857.85	-4464.88	-37.00
7132.55	90.40	180.20	3857.70	-4488.51	-37.00
7150.00	90.08	180.20	3857.63	-4505.96	-37.06
7198.16	89.20	180.20	3857.93	-4554.12	-37.23

References

[1] A.T.Bourgoyne, M.E.Chenevert, K.K. Millheimand F.S. Young, "Applied Drilling Engineering," *Society of Petroleum Engineering (SPE)*, 1986.

[2] Joshi, S. D. and W. Ding, "The Cost Benefits of Horizontal Drilling," *American Gas Association*, Arlington, VA, USA, 1991.

[3] Conti, P. F., "Controlled Horizontal Drilling," *Society of Petroleum Engineers International Association of Drilling Contractors Drilling Conference*, New Orleans, LA, USA, 1989.

[4] Fisher, E. K. and M. R. French, "Drilling the First Horizontal Well in The Gulf of Mexico: A Case History of East Cameron Block 278 well B-12," *Society of Petroleum Engineers Annual Technical Conference and Exhibition*, Dallas, TX, USA, 1991.

[5] E. van Oort, J.E. Friedheim, and B. Toups, "Drilling Faster with Water-Base Muds," AADE, Annual Technical Forum – Improvements in Drilling Fluids Technology, Houston, Texas, March 30-31, 1999.

[6] Ron Bland, Bill Haliday, Roland Illerhaus, Mat Isbell, Scott McDonald, and Rolf Pessier, "Drilling Fluid and Bit Enhancement for Drilling Shales," AADE, Annual Technical Forum – Improvements in Drilling Fluids Technology, Houston, Texas, March 30-31, 1999.

[7] George D. Combs, "Prediction of Pore Pressure from Penetration Rate," SPE 2162, Society of Petroleum Engineering AIME, Dallas, TX, 1968.

[8] Helm, W., "Method and Apparatus for Measurement of Azimuth of a Borehole While Drilling," US patent # 5012412, 1991.

[9] Thorogood, J. L. and D. R. Knott, "Surveying Techniques with A Solid State Magnetic Multi-Shot Device," Society of Petroleum Engineers Drilling Engineering, V5 (3), pp: 209-214, 1990.

[10] Russel, M. K. and A. W. Russel, "Surveying of Boreholes," *US patent # 4163324,* 1979.

[11] R.W.Tucker and C. Wang, "An integrated model for drill string dynamics," *Journal of Sound and Vibration* 224(1), 123-165, 1999.

[12] Benjamin P. Jeffryes, "Determination of Drill Bit Rate of Penetration from Surface measurements," *USA Patent 5398546, Schlumberger Technology Corporation,* 1995

[13] Hyun Cho and S.O. Osisanya, "Application of Specific Energy Concept For Interpreting Single Polycrystalline Diamond Compact (PDC) Bit Rock Drilling Interaction," *School of Petroleum and Geological Engineering The University of Oklahoma,* 2001

[14] Arthur Lubinski, "Instantaneous Bit Rate of Drilling Meters," *USA Patent* 2688871, 1949.

[15] Jean-Hubert Guignard, "Methods and Apparatus for Measuring the Rate of Penetration in Well Drilling," *USA Patent 3777560, Schlumberger Technology Corporation,* 1973.

[16] David S. K. Chan, "Method and Apparatus for Measuring the Depth of a Tool in a Borehole," *USA Patent 4545242, Schlumberger Technology Corporation,* 1985.

[17] Yves Kerbart, "Procedure for Measuring the Rate of Penetration of a Drill Bit," *USA* Patent 4843875, Schlumberger Technology Corporation, 1989.

[18] I.G. Falconer, T.M. Burgess, and M.C. Sheppard, "Separating Bit and Lithology Effects from Drilling Mechanics Data," IADC/SPE 17191, Drilling Conference, Dallas, TX, February 1988.

[19] Matthew Bible, Marc Lesage, and Ian Falconer, "Method for Detecting Drilling Events from Measurement While Drilling Sensors," USA Patent 4876886, Anadrill Inc., 1989.

[20] R.C. Pessier, and M.J. Fear, "Quantify Common Drilling Problems with Mechanical Specific Energy and a Bit-Specific Coefficient of Sliding Friction," SPE 24584, 67th Annual Technical Conference and Exhibition of Society of Petroleum Engineers, Washington, DC, October 4-7, 1992.

[21] John Rogers Smith and Jeffrey Bruce Lund, "Single Cutter Tests Demonstrate Cause of Poor PDC Bit Performance in Deep Shales," ETCE 2000, ASME - Drilling Technology Symposium, Houston, TX, February 14-17, 2000.

[22] John Rogers Smith, "Performance Analysis of Deep PDC Bits Runs in Water-Base Muds," ETCE 2000, ASME - Drilling Technology Symposium, Houston, TX, February 14-17, 2000.

[23] Charles H. King and Mitchell D. Pinckard, "Method of and System for Optimizing Rate of Penetration in Drilling Operations," USA Patent 6026912, Noble Drilling Services Inc., 2000

[24] Charles H. King, Mitchell D. Pinckard, Kalimuthu Krishnamoorthy, and Denise F. Benton, "Method of and System for Optimizing Rate of Penetration in Drilling Operations," USA Patent 6155357, Noble Drilling Services Inc., 2000.

[25] Conn William Michael, Ott Eugene Gray, "Insert cutter for cutting kerfs," US Patent No. 3858670 A, 1975.

[26] Ruhle James L, " Method of drilling oil wells," US Patent No. 3692125 A, 1972.

[27] Kenneth W. Jones, "Oil well drilling bit," US Patent No. 4420050, Reed Rock Bit Company, 1983.

[28] David Dardick," Directional drilling," US Patent No. 4582147,Tround International, Inc., 1986.

[29] Macmillan M. Wisler, Jian-gun Wu, "Method for drilling directional wells," US Patent No. 5230386, Baker Hughes Incorporated, 1993.

[30] Michael C. Thompson, "Method and apparatus for forming lateral boreholes," US Patent No. 5425429, 1995.

[31] William C. Saxman, "Drill bit with improved rolling cutter tooth pattern," US Patent No. 5429201, Dresser Industries, Inc., 1995.

[32] Thomas C. Gipson, "Method and system for downhole redirection of a borehole," US Patent No. 5439066 Fleet Cementers, Inc., 1995.

[33] Michael D. Hathaway, " Horizontal drilling apparatus," US Patent 5553680, 1996.

[34] Neal A. Kuenzi, Rodney R. Kuenzi, "Drill bit for directional drilling," US Patent 6308789, 2001.

[35] Michael Gerald Smith, Melvin Flois Hicks, "Apparatus for directional drilling," US Patent No. 6386298, 2002.

[36] Marc Haci, Eric E. Maidla, "Method of and apparatus for directional drilling," US Patent No. 6802378, Noble Engineering And Development, Ltd., 2004.

[37] Stephen John McLoughlin, Jeffrey B. Lasater, Jack P. Chance, George B. Sutherland, Feroze M. Variava, Emerson Marcellus, "Wellbore directional steering tool," US Patent No. 6808027 Rst (Bvi), Inc., 2004.

[38] John B. Sved, "Steerable horizontal subterranean drill bit," US Patent No. 6810971 Hard Rock Drilling & Fabrication, L.L.C., 2004.

[39] Scott Christopher Adam, Timothy Gregory Hamilton Meyer, "Drill head steering," US Patent No. 7195082, 2007.

[40] Michael King Russell, Colin Walker, "Directional drilling control," US Patent No. 7543658, Russell Oil Exploration Limited, 2009.

[41] Mohsin Hamed Al Hadhrami, "Method and apparatus for three dimensional geosteering," US 7958949, Schlumberger Technology Corporation, 2011.

[42] P. L. Moore, "Drilling Practices Manual. Petroleum Publishing Company", Tulsa, OK, U.S.A.,1974.

[43] R. TEALE, "The Concept of Specific Energy in Rock Drilling," *Int. J. Rock Mech. Mining Sciences,* Vol. 2, pp. 57-73, 1972.

[44] Walker D. R. and Shaw M.C. *Mining Engineering 6,* 313-20, 1954. Pergamon Press 1965.

[45] Anthony K. Booer, "Determination of Drill Bit Rate of Penetration from Surface Measurements,"*USA Patent 5551286, Schlumberger Technology Corporation,*1996.

[46] John W. Harrell, Vladimir Dubinsky, and James V.Leggett III, "Closed Loop Drilling System," *USA Patent 5842149, Baker Hughes Inc.,* 1998.

[47] S. F. Chien, "Annular Velocity for Rotary Drilling Operations. In Proceedings of SPE Fifth Conference on Drilling and Rock Mechanics", Jan. 5-6, 1971, pages 5–16. *Society of Petroleum Engineers (SPE),* Austin, TX, U.S.A., 1971.

[48] Spanos P.D., Sengupta A.K., Cunningham R.A., and Paslay P.R. "Modeling of roller cone bit lift-off dynamics in rotary drilling," *Journal of Energy Resources Technology,* 117(3):197–207, 1995.

[49] Dunlop,J., Isangulov, R., Aldred, W., Arismendi Sanchez, H., Sanchez Flores, J.L.,Alarcon Herdoiza, J.,Belaskie, J.,Luppens, J.C., "Increased Rate of Penetration Through Automation," *SPE/IADC* 139897.2011.

[50] Ho, H.S.," Prediction of Drilling Trajectory in Directional Wells Via a New Rock-Bit Interaction Model," *SPE* 16658, 1987.

[51] Rashidi, B., Hareland, G. and Nygaard.R, "Real-Time Drill Bit Wear Prediction by Combining Rock Energy and Drilling Strength Concepts", *Abu Dhabi international Petroleum Exhibition and Conference,* SPE117109, 2008.

[52] Rashidi, B., et al., "Real-Time Bit Wear Optimization Using the Intelligent Drilling Advisory System", *SPE Russian Oil and Gas Conference and Exhibition, Society of Petroleum Engineers: Moscow, Russia.*2010.

[53] Moses, A.Alum and F.Egbon "Semi-Analytical Models on the Effect of Drilling Fluid Properties on Rate of Penetration (ROP)", *Nigeria Annual International Conference and Exhibition,Society of Petroleum Engineers,* 30 July - 3 August 2011.

[54] García Carrillo**,** L.R**.,** DzulLópez**,** A.E**.,**Lozano**,** R.,Pégard**, "**Quad Rotorcraft Control," *XIX,* 179 p. 117 illus., 74 illus. in color, ISBN 978-1-4471-4399-4.2013.

[55] Matthew Bible, Marc Lesage, and Ian Falconer, "Method for Detecting Drilling Events from Measurement While Drilling Sensors," *USA Patent 4876886, Anadrill Inc.,* 1989

[56] Bak, T., "Modeling of Mechanical Systems", *Lecture Notes- AAU,* 1-edition, 2002.

[57] Maurer, W. C.: "The 'Perfect Cleaning' Theory of Rotary Drilling," *Pet. Tech. 12701274; Trans., AIME,* Vol. 225.Nov. 1962.

[58] Vidrine, D. J., and Denit, E. J.: "Field Verification of the Effect of Differential Pressure on Drilling Rate," *J .Pet. Tech.* 676-682, July 1968.

[59] Eckel, J. J.: "Micro-bit Studies of the Effect of Fluid Properties and Hydraulics on Drilling Rate," *J .Pet. Tech*. 541-546; Trans., AIME, Vol. 240.April 1967.

[60] Murray, A. S., and Cunningham, R. A.: "The Effect of Mud Column Pressure on Drilling Rates," *Trans., AIME* Vol. 204, 196-204.1955.

[61] J. Chiasson, "Dynamic feedback linearization of the induction motor," IEEE Trans. Automat. Contr., vol. 38, pp. 1588–1594, Oct. 1993.

[62] J. Chiasson and M. Bodson, "Nonlinear control of a shunt DC motor," IEEE Trans. Automatic Contr., vol. 38, pp. 1662–1665, Nov. 1993.

[63] W. Leonhard, Control of Electrical Drives. New York: Springer-Verlag, 1990.

[64] C. T. Chen, "Linear System Theory and Design," *Oxford University Press*, 3/e, 1999.

[65] Slotine, J.J.E., and Li, W.," Applied Nonlinear Control*,"* Prentice-Hall, 1991.

[66] Freddi A, Lanzon A, and Longhi S, "A feedback linearization approach to fault tolerance in quadrotor vehicles", *In 18th IFAC World Congress*.

[67] MAO Jr.Alves, E Nobrega, and T.Yoneyama, "Adaptive neural control for a tolerant fault system", *In 7th IFAC Symposium on Fault Detection, Supervision and Safety of Technical Processes*, pages 137–142.

[68] C.Berbra, S.Lesecq, and J.J.Martinez, "A multi-observer switching strategy for fault-tolerant control of a quadrotor helicopter", *In Control and Automation, 2008 16th Mediterranean Conference on*, pages 1094– 1099.

[69] S.Bouabdallah, M.Becker, and R.Siegwart, "Autonomous miniature flying robots-research, development, and results", *Robotics and Automation Magazine*, IEEE, 14(3):88–98, 2007.

[70] O. Bourquardez, R.Mahony, N.Guenard, F.Chaumette, T.Hamel, and L.Eck, "Image-based visual servo control of the translation kinematics of a quadrotor aerial vehicle", *Robotics,* IEEE Transactions on, 25(3):743– 749, 2009.

[71] P.Castillo, A.Dzul, and R.Lozano, "Real-time stabilization and tracking of a four-rotor mini rotorcraft. Control Systems Technology", *IEEE Transactions on*, 12(4):510–516, 2004.

[72] A. Das, K. Subbarao, and F. Lewis, "Dynamic inversion with zero dynamics stabilization for quadrotor control", *Control Theory and Applications*, IET, 3(3):303–314, 2009.

[73] Abhijit Das, Frank Lewis, and Kamesh Subbarao, "Backstepping approach for controlling a quadrotor using lagrange form dynamics", *Journal of Intelligent and Robotic Systems*, 56(1):127–151, 2009.

[74] L. Derafa, A. Benallegue, and L. Fridman, “Super twisting control algorithm for the attitude tracking of a four rotors UAV”, Journal of the Franklin Institute, 349(2):685–699, 2012.

[75] Stoner Engineering Services (SES), version 4.5, stoner engineering LLC, 1999-2010.

Vitae

Name	: Mohammad Talib
Nationality	: Indian
Date of Birth	:7/13/1988
Email	: mohammadt94@yahoo.in
Address	: #27-7-3, K.V.Thota 3rd Lane, Guntur-522004, India.
Academic Background	: Master of Science, Automation and Control King Fahd University of Petroleum and Minerals, Dhahran Kingdom of Saudi Arabia.